Electronic Supplementary Information (ESI) for:

High-spin, tetrahedral cobalt(II) and nickel(II) complexes supported by monoprotic aminophosphine ligands, and attempted extension to copper(II) complexes: synthesis, characterization, and unexpected reactivity

Jordan C. Kelly[†] and Aaron J. Bloomfield*[†]

[†]Department of Chemistry and Biochemistry, Duquesne University, Pittsburgh, Pennsylvania 15282

Contents

Experimental Details

Materials

All reagents were used as received unless otherwise stated: 2-picolylamine (TCI, 98+%), 2-(2-aminoethyl)pyridine (TCI, 98+%), t-butyldichlorophosphine (Strem Chemicals Inc., 98%) nickel(II) chloride, dimethoxyethane adduct (Stream Chemicals Inc., 97%), anhydrous cobalt (II) chloride (Alfa Aesar, 99.7%), and anhydrous copper (II) chloride (Alfa Aesar, 98+%). Triethylamine (VWR) was further purified before use. The reagent was first degassed using freeze-pump-thaw (FPT) cycling. Then, calcium hydride was added and allowed to dry overnight. The next day, the solution was FPT cycled and distilled. Tetrahydrofuran (Macron) was freshly distilled from a mixture of sodium metal and benzophenone, and FPT cycled immediately before use.

Instrumentation

^{1}H, ^{13}C, and ^{31}P NMR spectra were obtained from a Bruker Avance II 400 MHz spectrometer. ^{1}H and ^{13}C NMR chemical shifts were referenced to the residual hydrogen and carbon signals, respectively, of deuterated chloroform. ^{31}P NMR chemical shifts were internally referenced to a H_3PO_4 (85%) capillary. UV-Vis spectra were collected from a Cary 100 Series spectrophotometer from Agilent Technologies operating at 190-900 nm. Single Crystal XRD measurements were collected from a Bruker Smart Apex II CCD diffractometer operating at 273(2) K using graphite-monochromated Mo-K (λ_α = 0.71073 Å) radiation. The structures were solved using a multi-scan method (SADABS) and refined by full-matrix least-squares technique (SHELXTL 6.1). Molecular crystal structure images were processed through CrystalMaker. Solid-state UV-Vis near-IR data were collected with a Varian Cary 5000 UV-Vis-NIR spectrophotometer using a diffuse reflectance accessory. Scanning at a rate of 600 nm/min, data were collected from 2500 to 200 nm. All samples were measured with $BaSO_4$ (Fisher Scientific, 99.92%) as the 100% reflectance standard. For data acquisition, samples were ground and pressed on top of the reference that was preloaded in the sample cup. The Kubelka-Munk equation was used to convert reflectance data to absorption.

Synthesis and Complexation

Syntheses were conducted under an inert atmosphere of nitrogen using Schlenk line techniques, with glassware dried at 150°C overnight, and solvents that were FPT cycled unless otherwise stated. Glassware and syringes were purged with nitrogen for fifteen minutes before use.

2. *1,1-di(tert-butyl)-N-(pyridin-2-ylmethyl)phosphanamine.* A 50 mL bomb flask was purged, then charged with 2-picolylamine (1.29 mL, 12.5 mmol) and tetrahydrofuran (25 mL, 0.50 M). Next, triethylamine (1.74 mL, 12.5 mmol) was added. Then, di(*tert*-butyl)phosphine chloride (2.38 mL, 12.5 mmol) was added dropwise. The mixture stirred for 22 hours. The reaction mixture was filtered through a fine glass frit and volatiles were removed under vacuum, resulting in a yellow oil. Due to the sensitivity of the ligand to oxidize and decompose, further purification was not conducted. The oil was dissolved in tetrahydrofuran (25 mL, 0.50 M) and used for metal complexation. A single crystal of the oxidized ligand **2=O** was prepared by washing the reaction solution with *n*-pentane. ^{1}H NMR (400 MHz, $CDCl_3$): δ = 8.54 (d, 1H, J = 4.8 Hz py^6), 7.64 (t, 1H, J = 7.6 Hz py^4), 7.38 (d, 1H, J = 7.7 Hz py^3), 7.14 (t, 1H, J = 4.9 Hz py^5), 4.29 (d, 2H, J =

5.5 Hz, CH_2), 2.03 (b, 1H, N*H*), 1.11 and 1.08 [2s, 9H each, C(CH_3)$_3$]. $^{13}C\{^1H\}$ NMR (100 MHz, $CDCl_3$): δ = 161.86 (d, J = 1.5 Hz, py^2), 149.18 (d, J = 1.5 Hz, py^6), 136.54 (s, py^4), 121.79 (d, J = 3.3 Hz, py^5), 117.4 (s, py^3), 56.56 (d, J = 29.4 Hz, *C*H_2), 34.34 [d, J = 19.1 Hz *C*(CH3)3], 28.50 and 28.35 [2s, C(*C*H_3)$_3$] ppm. $^{31}P\{^1H\}$ NMR (160 MHz, $CDCl_3$): δ = 83.15 ppm.

2a. *Dichloro(1,1-di(tert-butyl)-N-(pyridine-2-ylmethyl)phosphanamine)cobalt.* **2** in tetrahydrofuran (5 mL, 0.50 M) was added to anhydrous $CoCl_2$ (0.3246 g, 2.5 mmol) and allowed to stir overnight. No color change was observed, however, peaks were no longer observable in the ^{31}P NMR spectrum because of the complex's paramagnetic character. The contents of the reaction flask were concentrated under reduced pressure, and *n*-pentane was added with stirring to crystallize a cobalt blue precipitate. The precipitate was collected on a fine glass frit and washed with diethyl ether. The solid was dried under vacuum to produce a cobalt blue solid in 58.9% yield (0.562 g). Elemental analysis found: C, 43.86; H, 6.50; N, 7.28%. Calculated for $C_{14}H_{25}Cl_2N_2CoP$: C, 44.00; H, 6.59; 7.33%.

2b. *Dichloro(1,1-di(tert-butyl)-N-(pyridine-2-ylmethyl)phosphanamine)nickel.* **2** in tetrahydrofuran (5 mL, 0.50 M) was added to $NiCl_2$(dme) (0.5495 g, 2.5 mmol) and allowed to stir. After one hour, a color change from orange to purple was observed indicative of ligand coordination. The solution stirred overnight to ensure the reaction was complete. Peaks were no longer observable in the ^{31}P NMR spectrum because of the complex's paramagnetic character. The contents of the reaction flask were concentrated under reduced pressure, and *n*-pentane was added with stirring to crystallize a dark purple precipitate. The precipitate was collected on a fine glass frit and washed with diethyl ether. The solid was dried under vacuum to produce a dark purple solid in 93.6% yield (0.894 g). Elemental analysis found: C, 43.69; H, 6.36; N, 7.01%. Calculated for $C_{14}H_{25}Cl_2N_2NiP$: C, 44.03; H, 6.60; 7.33%.

2b•HCl. HCl adduct of **2b** formed prior to ligand synthesis filtration. The purple solution when **2b** was dissolved in tetrahydrofuran or acetonitrile slowly transitioned to blue over the course of 4 days (Figure S31). Single crystals formed during slow evaporation indicated a zwitterion was formed as the ligand became monodentate and protonated while a third chloro substituent led to a negatively charged $NiCl_3$.

3. *1,1-di(tert-butyl)-N-(pyridin-2-ylethyl)phosphanamine.* A 50 mL bomb flask was purged, then charged with 2-(2-aminoethyl)pyridine (1.50 mL, 12.5 mmol) and tetrahydrofuran (25 mL, 0.50 M). Next, triethylamine (1.74 mL, 12.5 mmol) was added. Then, di(*tert*-butyl)phosphine chloride (2.38 mL, 12.5 mmol) was added dropwise. The mixture stirred for 22 hours. The reaction mixture was filtered through a fine glass frit and volatiles were removed under vacuum, resulting in a yellow oil. Due to the sensitivity of the ligand to oxidize and decompose, further purification was not conducted. The oil was dissolved in tetrahydrofuran (25 mL, 0.50 M) and used for metal complexation. ^1H NMR (400 MHz, $CDCl_3$): δ = 8.54 (d, 1H, J = 4.3 Hz py^6), 7.59 (t, 1H, J = 7.6 Hz py^4), 7.17 (d, 1H, J = 7.7 Hz py^3), 7.11 (t, 1H, J = 4.9 Hz py^5), 3.38 (t, 2H, J = 7.2 Hz, CH_2), 2.97 (t, 2H, J = 7.0 Hz, CH_2), 1.48 (b, 1H, N*H*), 1.03 and 1.00 [2s, 9H each, C(CH_3)$_3$]. $^{13}C\{^1H\}$ NMR (100 MHz, $CDCl_3$): δ = 160.66 (s, py^2), 149.50 (s, py^6), 136.54 (s, py^4), 123.58 (s, py^5), 121.33 (s, py^3), 50.60 (d, J = 29.9 Hz, *C*H_2), 42.11 (d, J = 6.9 Hz, *C*H_2), 34.09 [d, J = 18.4 Hz *C*(CH3)3], 28.46 and 28.32 [2s, C(*C*H_3)$_3$] ppm. $^{31}P\{^1H\}$ NMR (160 MHz, $CDCl_3$): δ = 79.03

ppm.

3a. *Dichloro(1,1-di(tert-butyl)-N-(pyridin-2-ylethyl)phosphanamine)cobalt.* **3** in tetrahydrofuran (10 mL, 0.50 M) was added to anhydrous $CoCl_2$ (0.649 g, 5.0 mmol) and allowed to stir overnight. No color change was observed, however, peaks were no longer observable in the ^{31}P NMR spectrum because of the complex's paramagnetic character. The contents of the reaction flask were concentrated under reduced pressure, and n-pentane was added with stirring to crystallize a cobalt blue precipitate. The precipitate was collected on a fine glass frit and washed with diethyl ether. The solid was dried under vacuum to produce a cobalt blue solid in 63.1% yield (1.250 g). Elemental analysis found: C, 45.04; H, 6.45; N, 6.65%. Calculated for $C_{15}H_{27}Cl_2N_2CoP$: C, 45.47; H, 6.87; 7.07%.

3b. *Dichloro(1,1-di(tert-butyl)-N-(pyridin-2-ylethyl)phosphanamine)nickel.* **3** in tetrahydrofuran (10 mL, 0.50 M) was added to $NiCl_2$(dme) (1.099 g, 5.0 mmol) and allowed to stir. After one hour, a color change from orange to purple was observed indicative of ligand coordination. The solution stirred overnight to ensure the reaction was complete. Peaks were no longer observable in the ^{31}P NMR spectrum because of the complex's paramagnetic character. The contents of the reaction flask were concentrated under reduced pressure, and n-pentane was added with stirring to crystallize a dark purple-blue precipitate. The precipitate was collected on a fine glass frit and washed with diethyl ether. The solid was dried under vacuum to produce a dark purple-blue solid in 92.0% yield (1.821 g). Elemental analysis found: C, 45.49; H, 6.23; N, 6.73%. Calculated for $C_{15}H_{27}Cl_2N_2NiP$: C, 45.50; H, 6.87; 7.07%.

4. A single crystal of **4** was obtained from crystallization of the transfer hydrogenation catalytic reaction solution involving **2b**, acetophenone, and potassium *tert*-butoxide in tetrahydrofuran and isopropanol. Ligand **2** reacted with residual BHT inhibitor in tetrahydrofuran to form **4**. Attempts to replicate these results in compounds **2a-b** and **3a-b** with one equivalent of BHT were unsuccessful.

5, 6, 7. Cu(II)-**3** complexes. **3** in tetrahydrofuran (5 mL, 0.50 M) was added to anhydrous $CuCl_2$ (0.336 g, 2.5 mmol) and allowed to stir overnight. The solution immediately turned from yellow to red with addition of ligand. With continuous stirring, the solution then turned a yellow-orange color. Finally, the solution began precipitating out a green solid after about 2 hours. The solution then became green with continuous stirring. Crystallizations were conducted with tetrahydrofuran-diethyl ether, and single crystals were obtained for the oxidized dimer (**5**) and oxidized coordination polymer (**6**). Additional crystallization attempts in methanol resulted in a monodentate complex (**7**) with a methoxy substituent on the phosphorus.

8. 2 in tetrahydrofuran was added to anhydrous $CuCl_2$ and allowed to stir overnight. The Cu(II) solution immediately turned from yellow to red with addition of ligand. With continuous stirring, the solution then turned a yellow-orange color. Finally, the solution began precipitating out a green solid after about 2 hours. The solution then became green with continuous stirring. Crystallizations were conducted with tetrahydrofuran-diethyl ether and single crystals were obtained showing zwitterionic complex of Cu(II) oxidized HCl adduct (**8**).

9. Stoichiometric reactivity studies were conducted with **3b** and $AgBF_4$ (1:1 molar ratio) in tetrahydrofuran. Crystallization of the ensuing solution resulted in colorless crystals of **9** and $AgCl_6$.

NMR Spectra

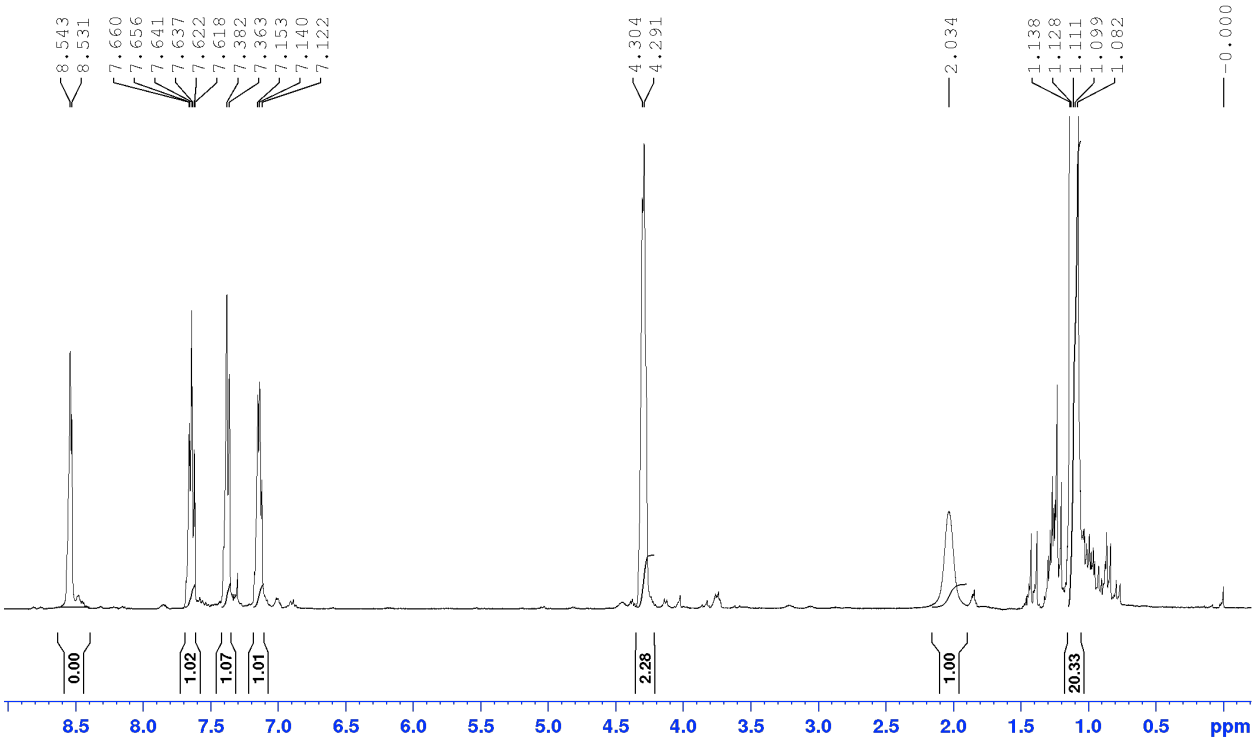

Figure S1: ^{1}H-NMR spectrum of ligand **2** in $CDCl_3$.

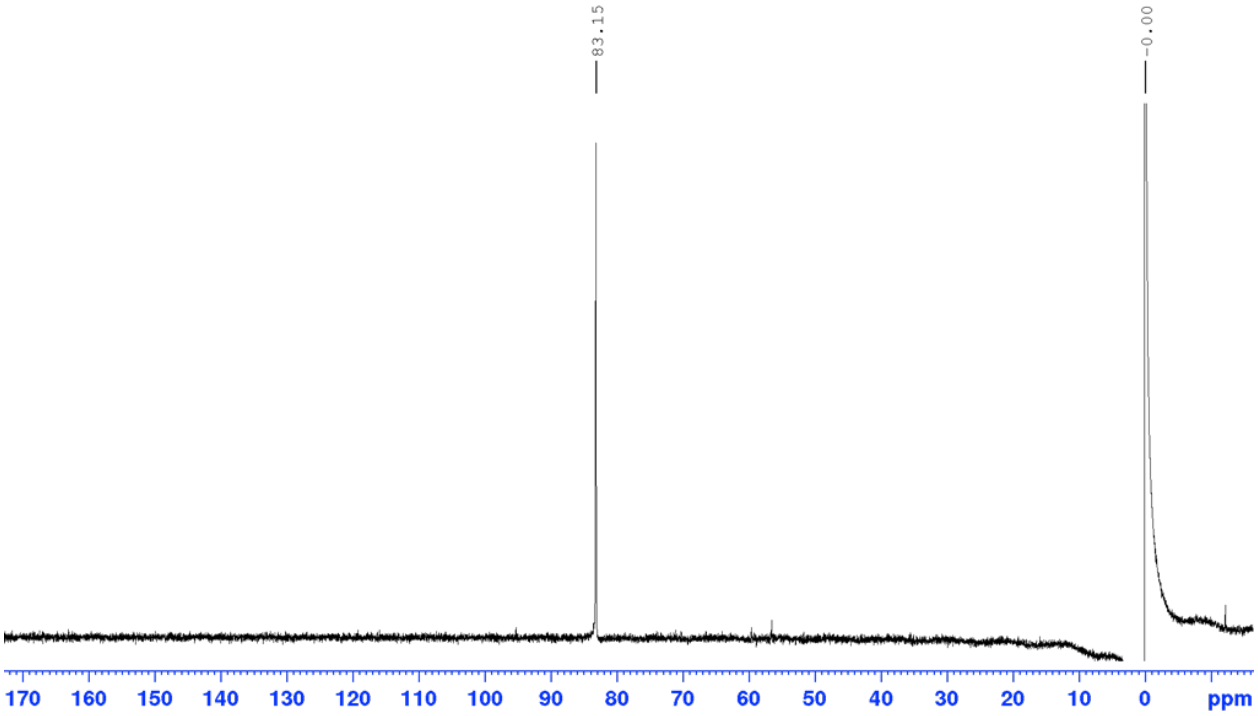

Figure S2: ^{31}P-NMR spectrum of ligand **2** in $CDCl_3$ with H_3PO_4 capillary.

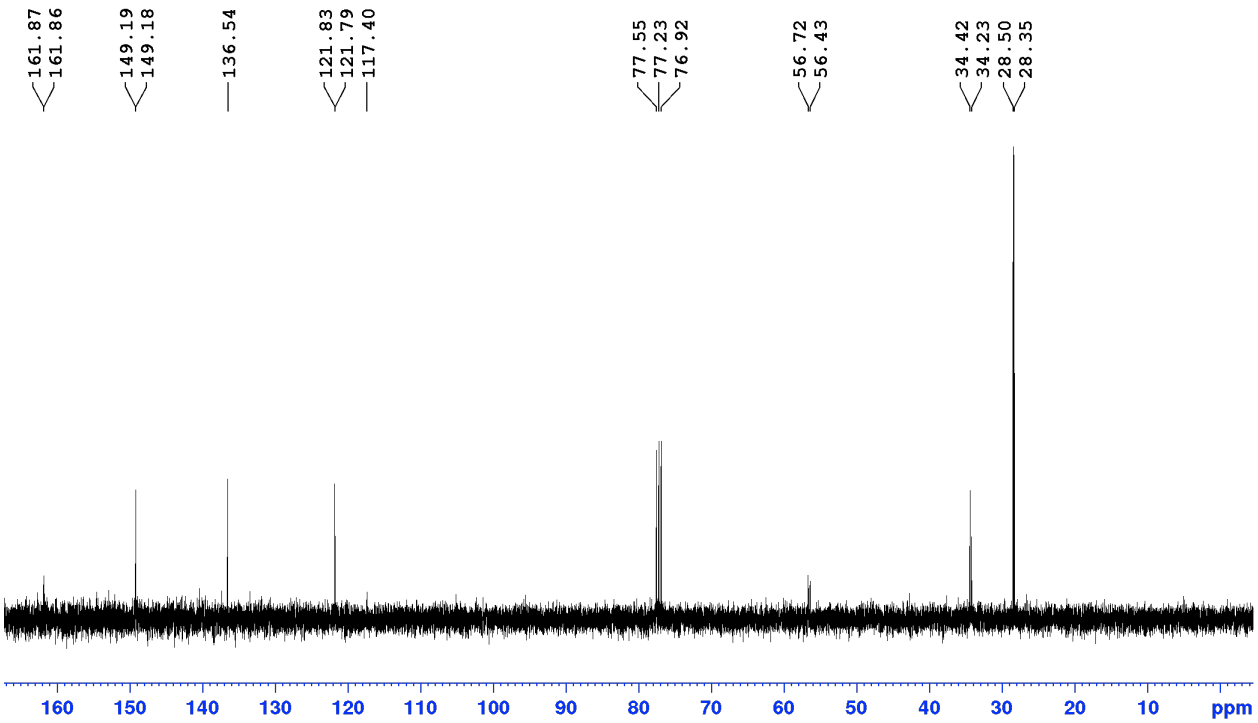

Figure S3: ^{13}C-NMR spectrum of ligand **2** in $CDCl_3$.

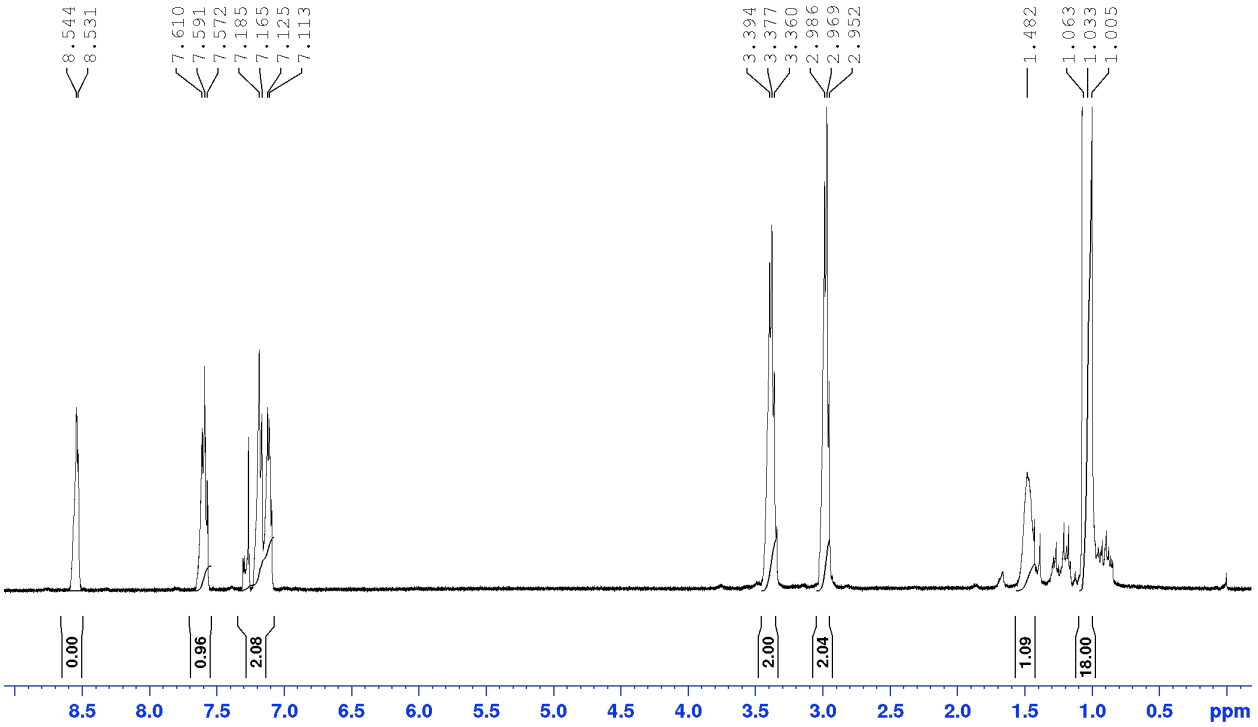

Figure S4: ^{1}H-NMR spectrum of ligand **3** in $CDCl_3$.

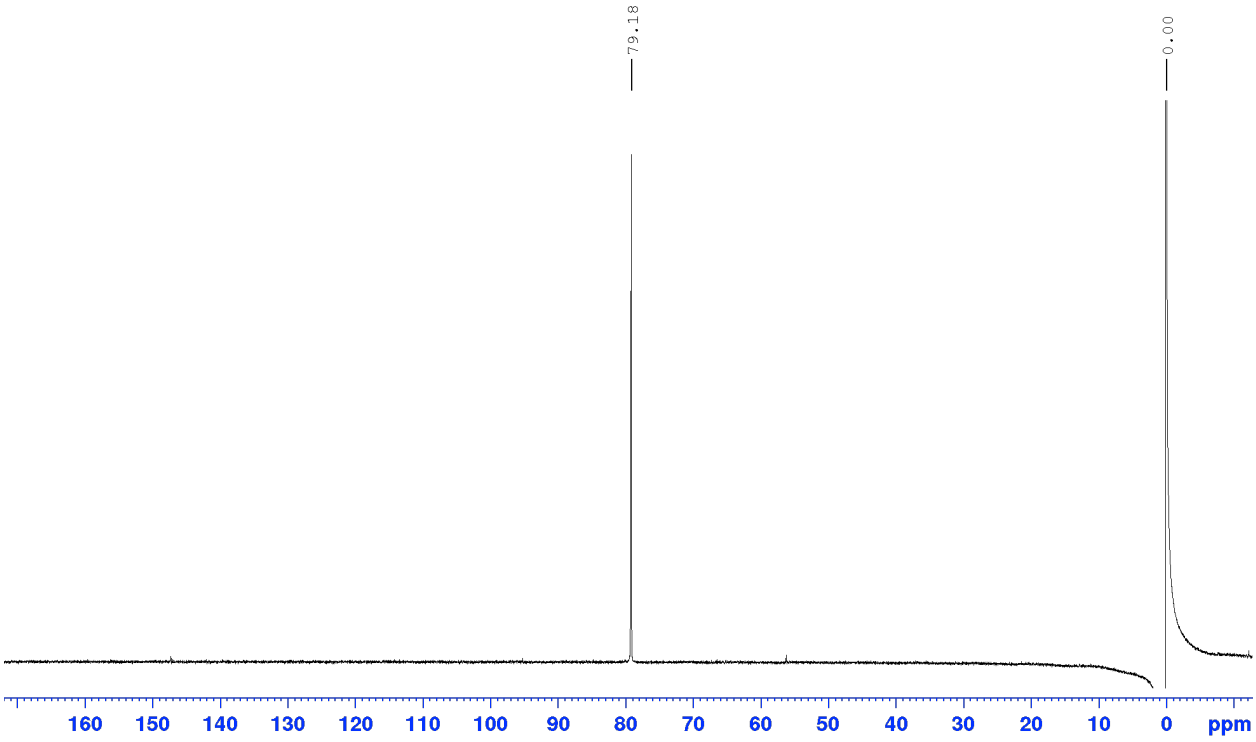

Figure S5: ^{31}P-NMR spectrum of ligand **3** in $CDCl_3$ with H_3PO_4 capillary.

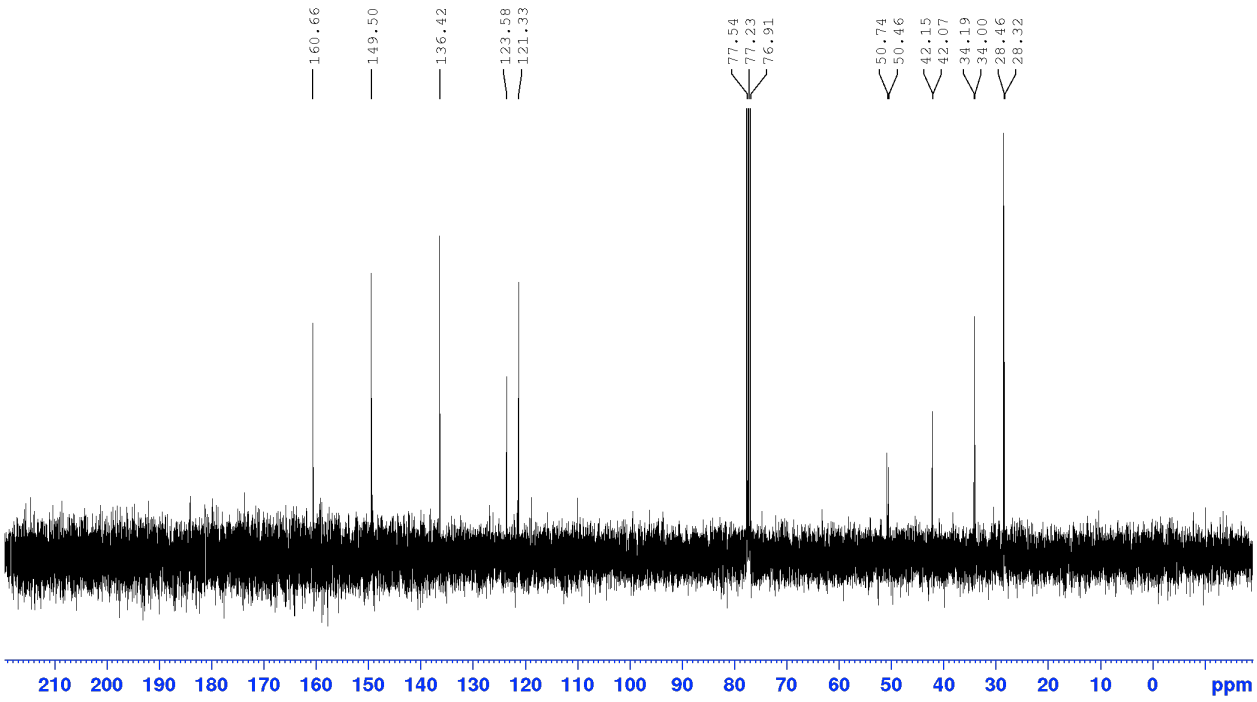

Figure S6: ^{13}C-NMR spectrum of ligand **3** in $CDCl_3$.

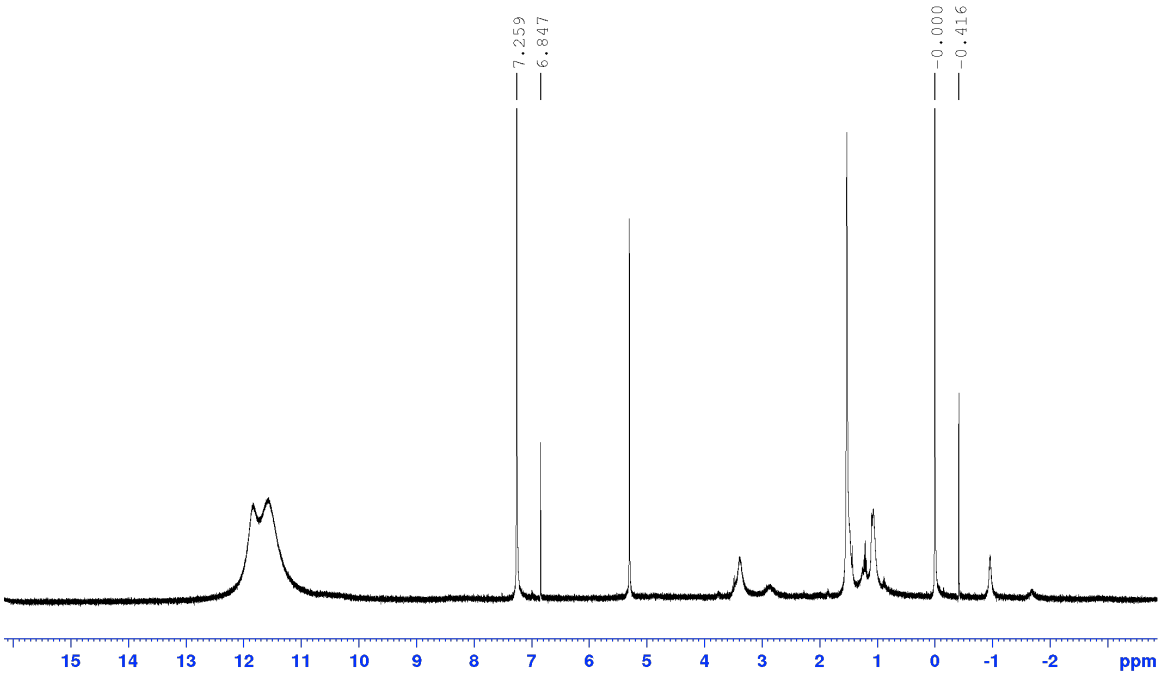

Figure S7: Evans Method, ^{1}H-NMR solution spectrum of Co(II) complex **2a** in $CDCl_3$ with a coaxially arranged capillary of $CDCl_3$.

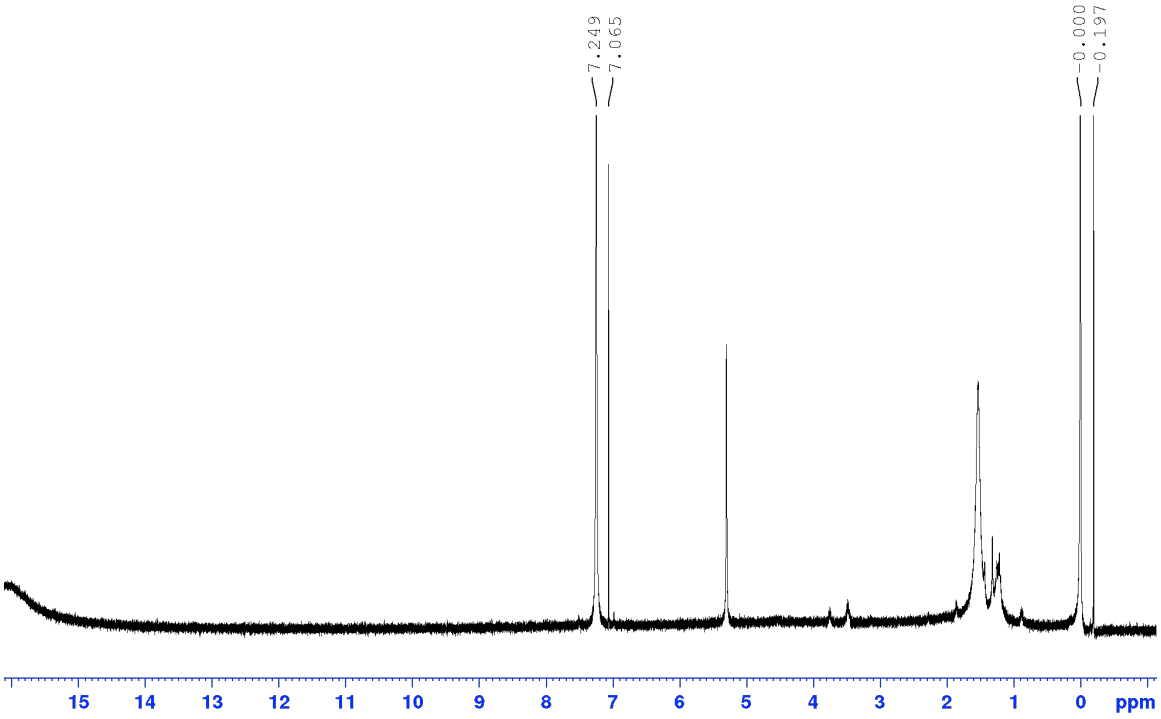

Figure S8: Evans Method, ^{1}H-NMR solution spectrum of Ni(II) complex **2b** in $CDCl_3$ with a coaxially arranged capillary of $CDCl_3$.

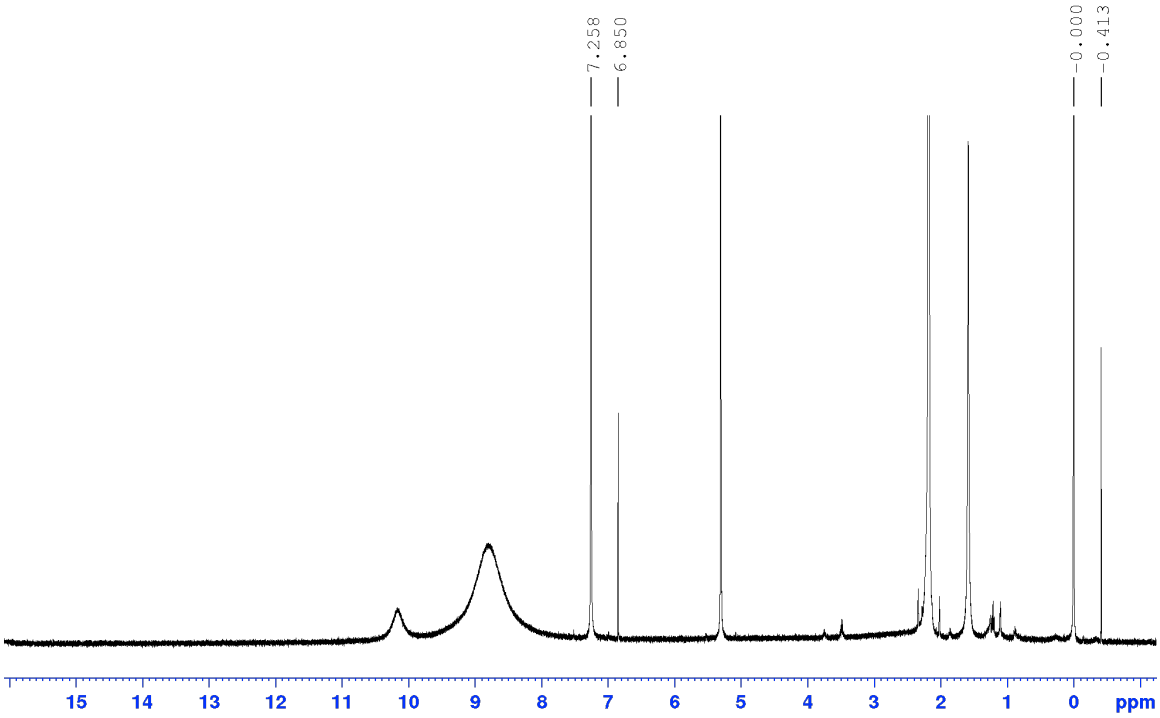

Figure S9: Evans Method, ^{1}H-NMR solution spectrum of Co(II) complex **3a** in $CDCl_3$ with a coaxially arranged capillary of $CDCl_3$.

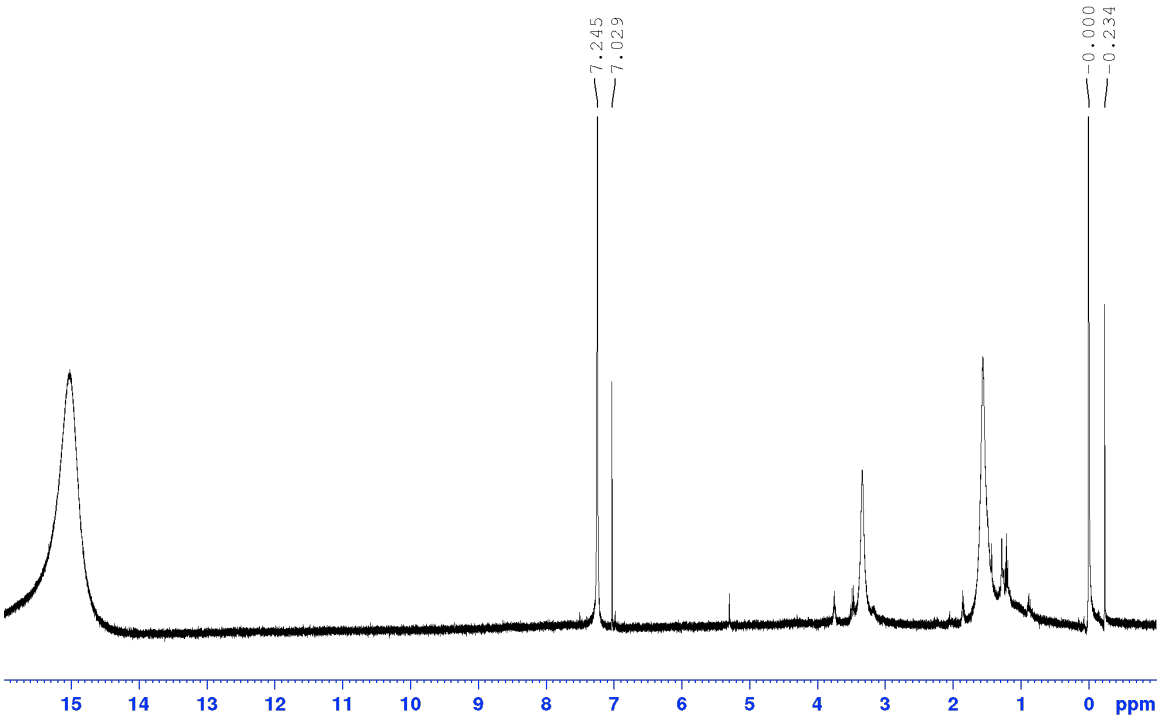

Figure S10: Evans Method, ^{1}H-NMR solution spectrum of Ni(II) complex **3b** in $CDCl_3$ with a coaxially arranged capillary of $CDCl_3$.

FTIR-ATR Spectra

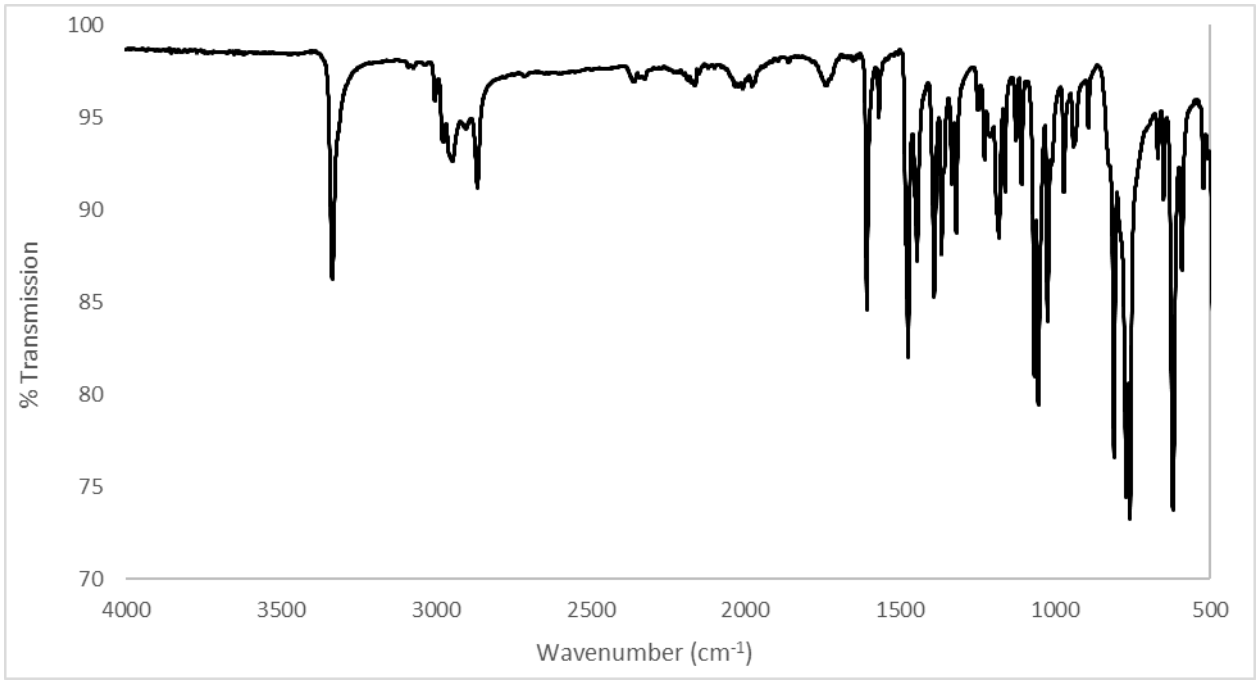

Figure S11: FTIR-ATR spectrum of Co(II) complex **2a**.

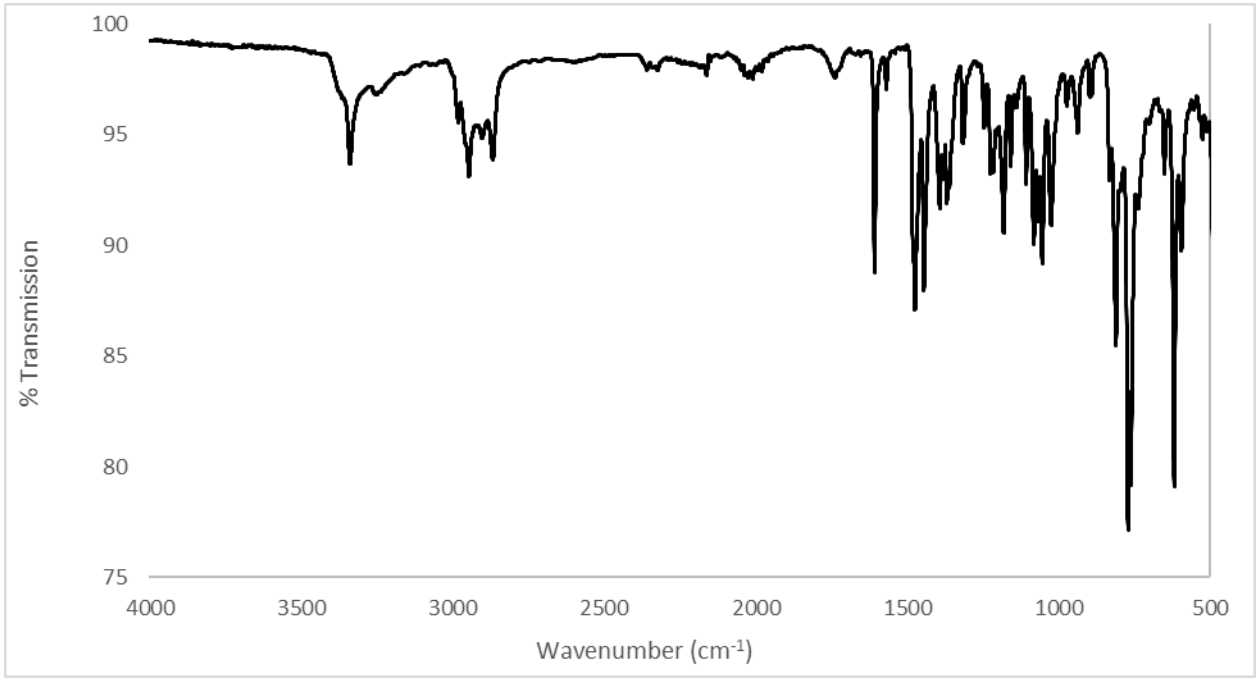

Figure S12: FTIR-ATR spectrum of Ni(II) complex **2b**.

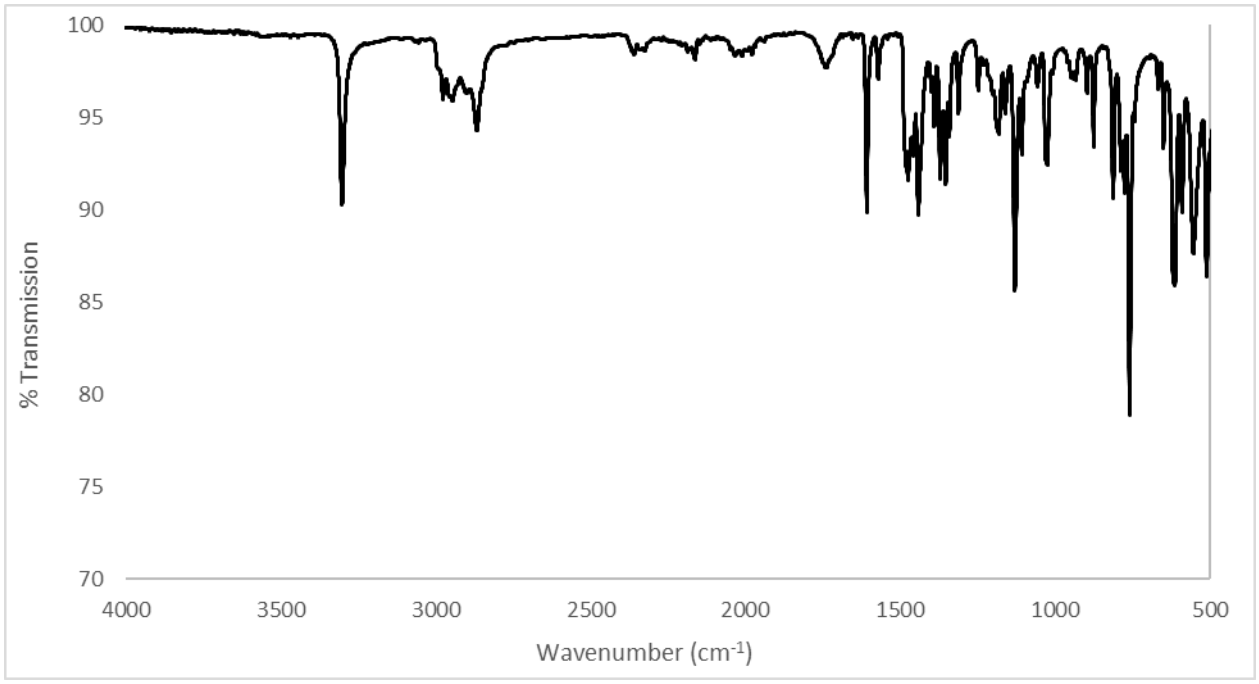

Figure S13: FTIR-ATR spectrum of Co(II) complex **3a**.

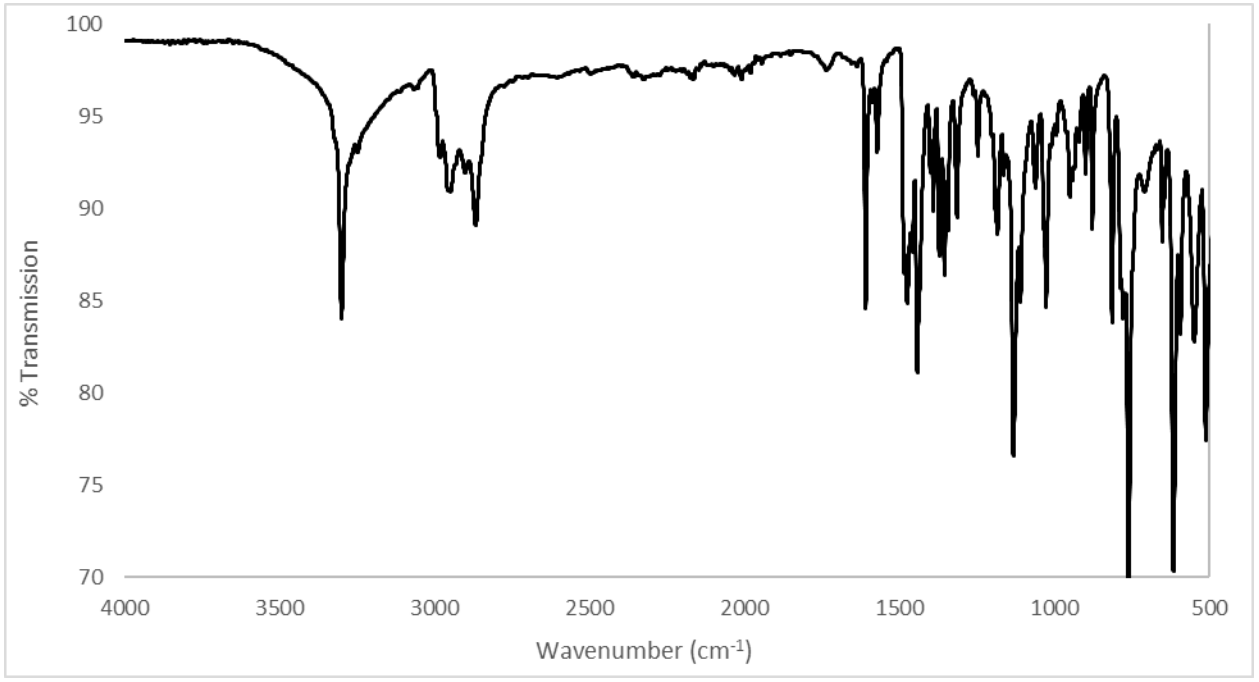

Figure S14: FTIR-ATR spectrum of Ni(II) complex **3b**.

Crystallographic Data

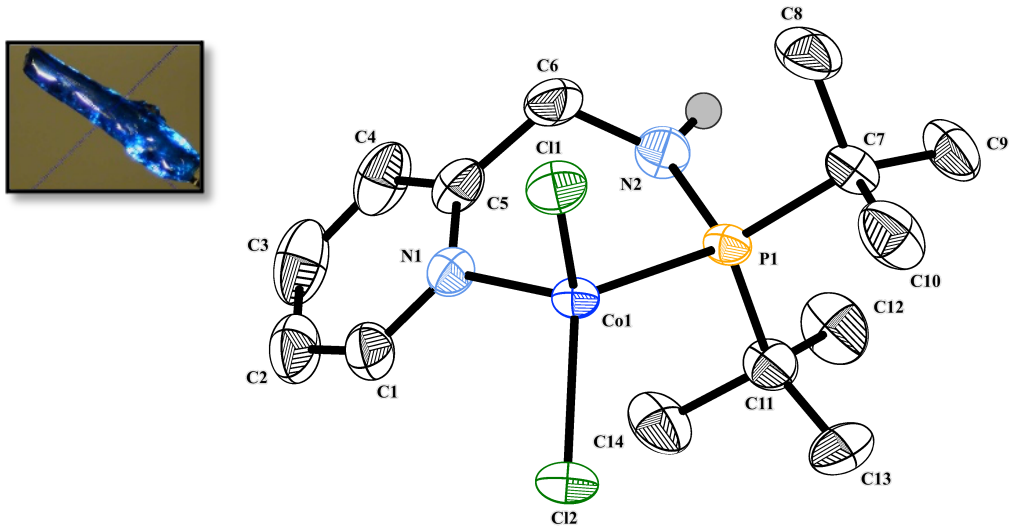

Figure S15: Structural view of Co(II) complex **2a** showing 40% thermal ellipsoids (carbon-bound hydrogen atoms emitted for clarity).

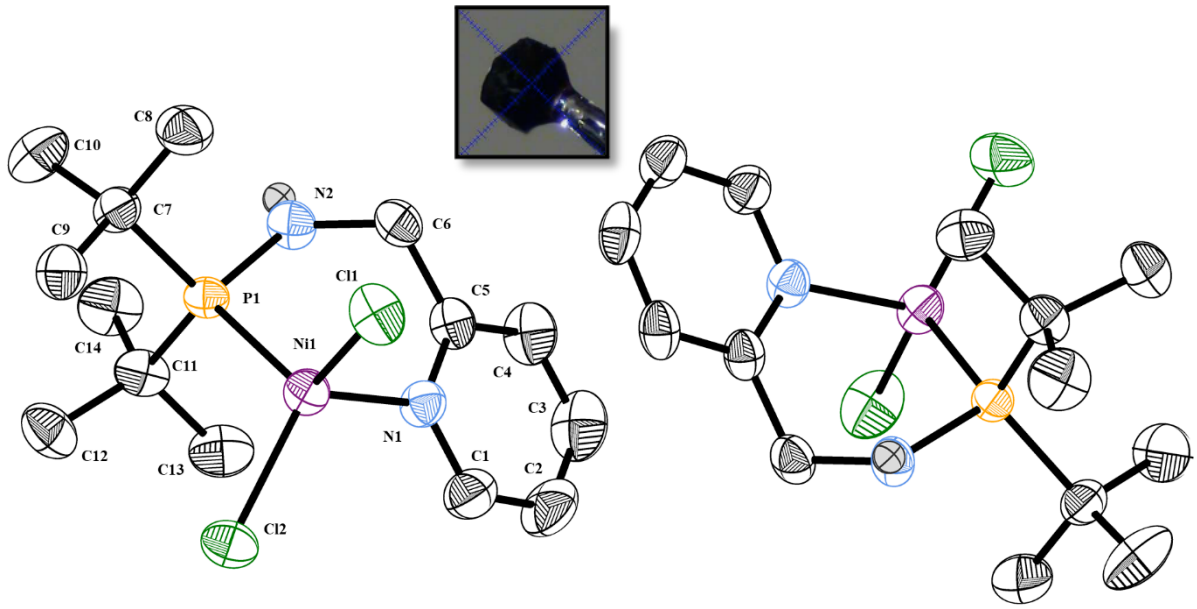

Figure S16: Structural view of Ni(II) complex **2b** showing 40% thermal ellipsoids (carbon-bound hydrogen atoms emitted for clarity).

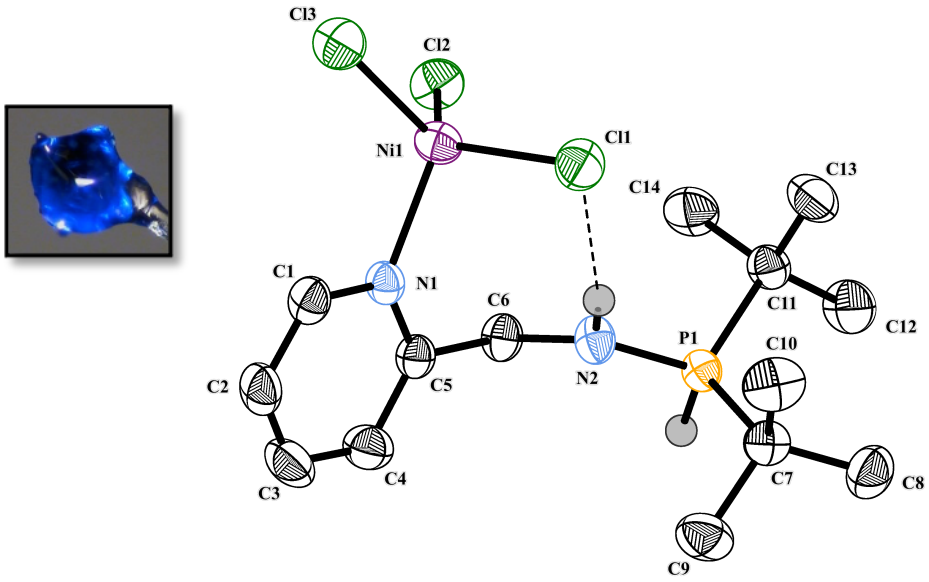

Figure S17: Structural view of HCl activated Ni(II) complex **2b•HCl** showing 40% thermal ellipsoids (carbon-bound hydrogen atoms emitted for clarity).

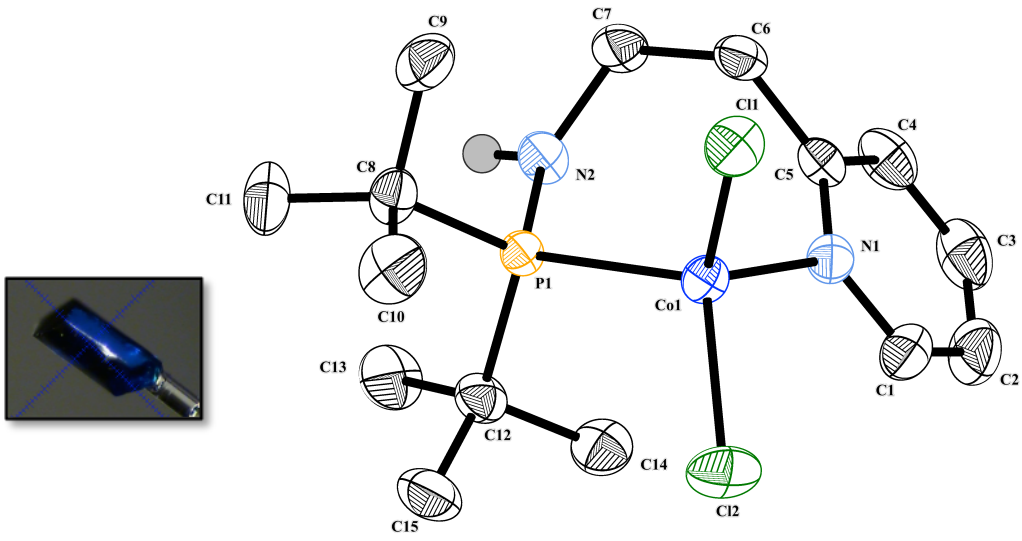

Figure S18: Structural view of Co(II) complex **3a** showing 40% thermal ellipsoids (carbon-bound hydrogen atoms emitted for clarity).

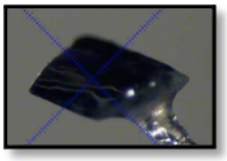

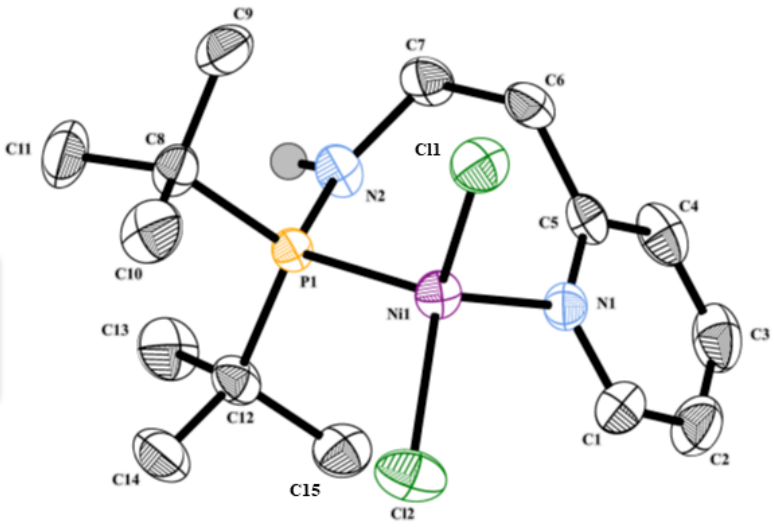

Figure S19: Structural view of Ni(II) complex **3b** showing 40% thermal ellipsoids (carbon-bound hydrogen atoms emitted for clarity).

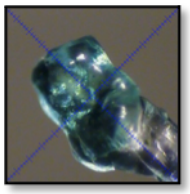

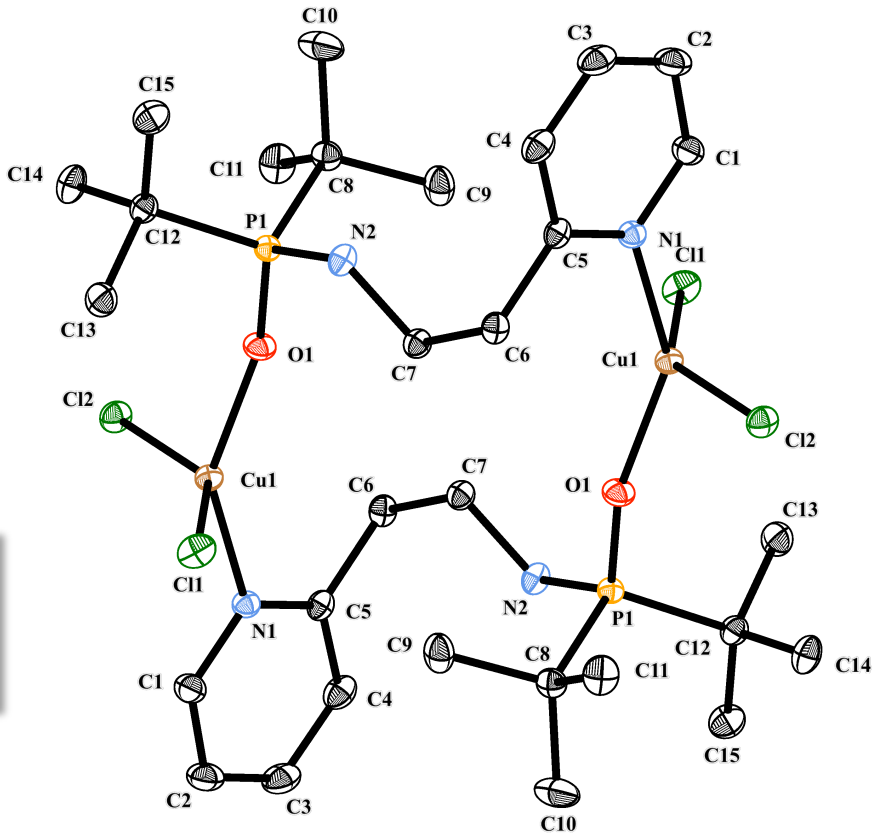

Figure S20: Structural view of Cu(II)-oxide dimer complex **5** showing 40% thermal ellipsoids (carbon-bound hydrogen atoms emitted for clarity).

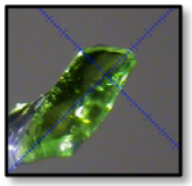

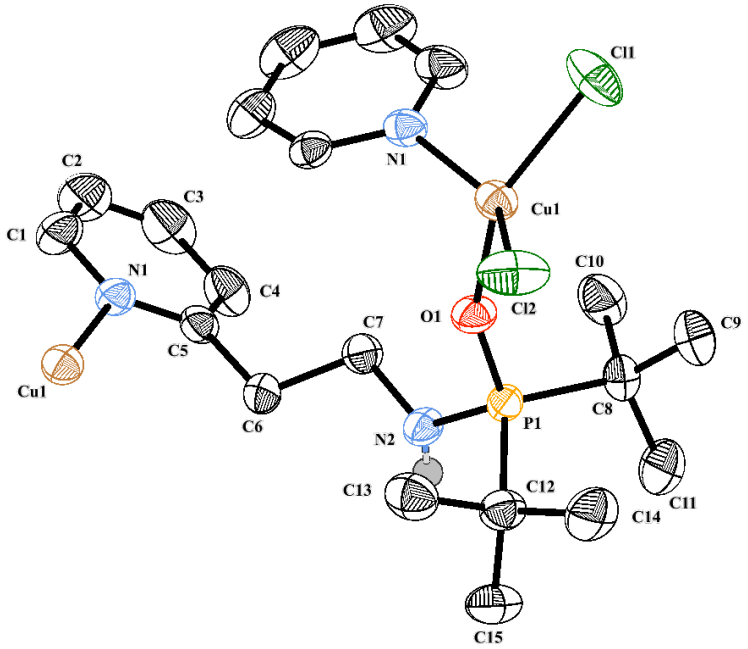

Figure S21: Structural view of Cu(II)-oxide coordination polymer **6** showing 40% thermal ellipsoids (carbon-bound hydrogen atoms emitted for clarity).

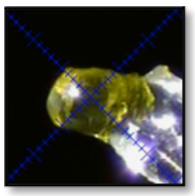

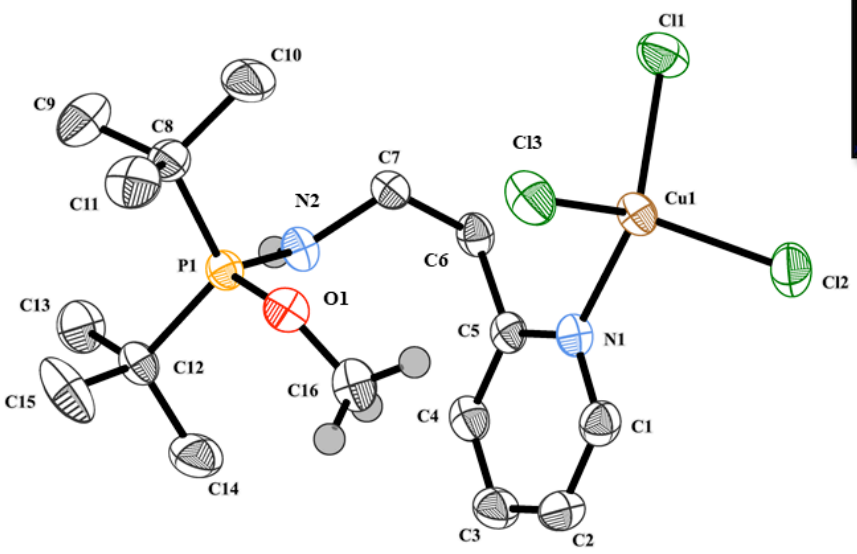

Figure S22: Structural view of Cu(II)-methoxy complex **7** showing 40% thermal ellipsoids (carbon-bound hydrogen atoms on ligand emitted for clarity).

Disordered Crystal Structures

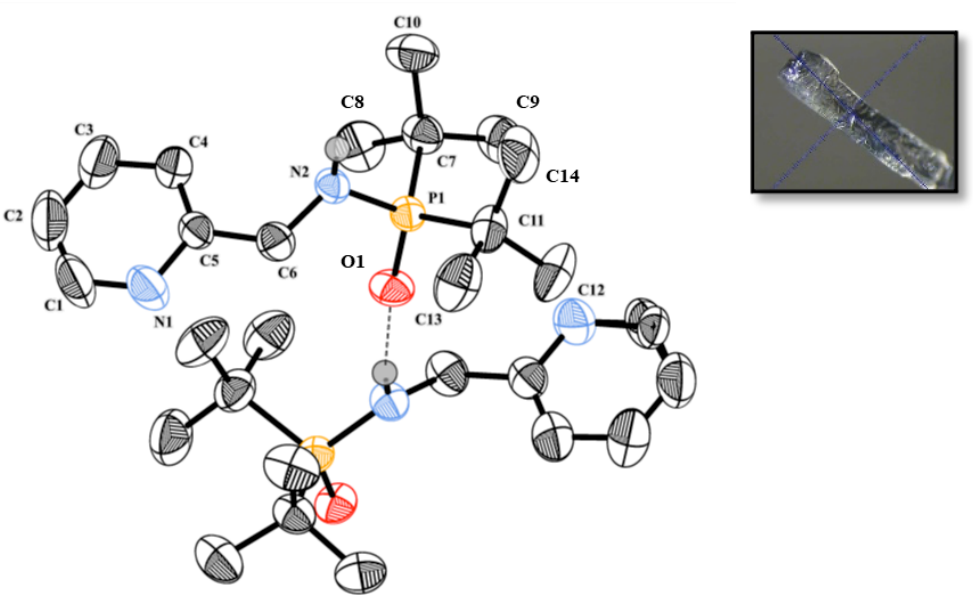

Figure S23: Structural view of oxidized ligand **2=O** showing 40% thermal ellipsoids (carbon-bound hydrogen atoms emitted for clarity).

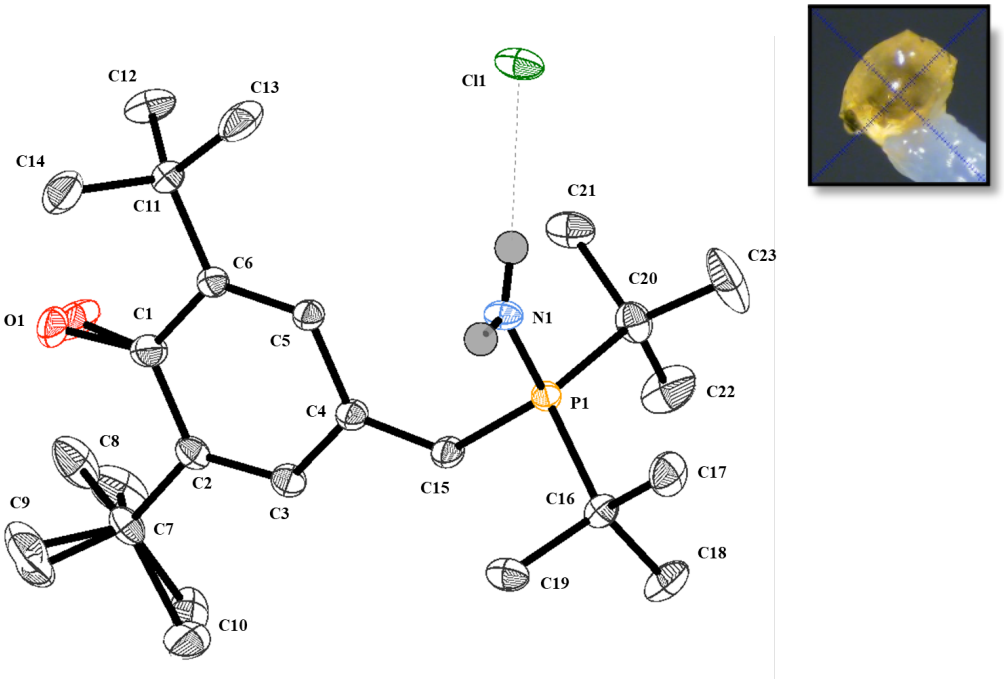

Figure S24: Structural view of BHT byproduct **4** showing 40% thermal ellipsoids (carbon-bound hydrogen atoms emitted for clarity). Selected bond lengths (Å): P—N 1.6111(8), O—C1 1.269(4), C1—C2 1.4880(14), C2—C3 1.3442(13), C3—C4 1.4560(12), C4—C15 1.3611(13), C15—P 1.7922(9).

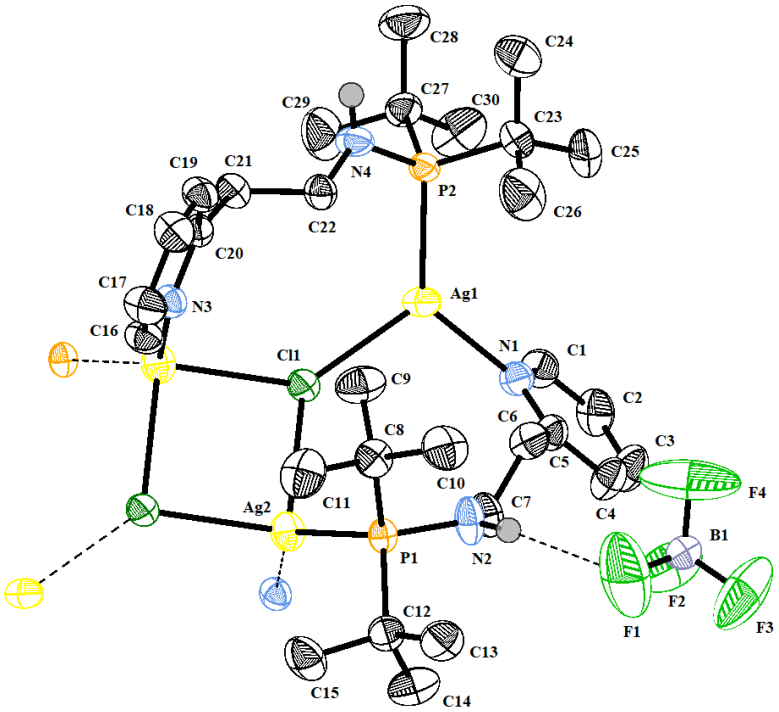

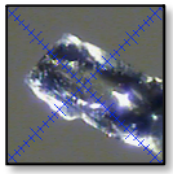

Figure S25: Structural view of $AgBF_4$ byproduct **10** showing 40% thermal ellipsoids (carbon-bound hydrogen atoms emitted for clarity). Selected bond lengths (Å): P—N 1.6550(16), 1.6590(15); Ag—N 2.3043(15), 2.3110(14); Ag—P 2.3858(5), 2.4142(4); Ag—Cl 2.5657(4), 2.7279(4), 2.9226(5). Selected angles (°) trigonal planar Ag: P-Ag-N 128.85(4), P-Ag-Cl 122.552(15), N-Ag-Cl 108.59(4). Selected angles (°) tetrahedral Ag: P-Ag-N 133.27(4), P-Ag-Cl 112.971(14), 108.115(15), N-Ag-Cl 89.70(4), 106.51(4).

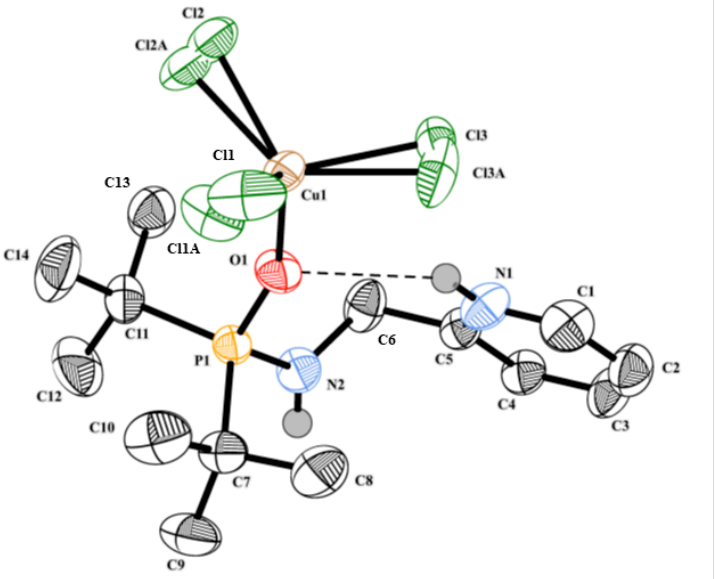

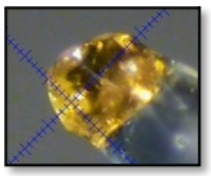

Figure S26: Structural view of Cu(II)-oxide complex **8** showing 40% thermal ellipsoids (carbon-bound hydrogen atoms emitted for clarity).

Table S1: Selected bond lengths (Å) and angles (°) for complexes **2a, 2b, 2b•HCl, 3a,** and **3b.**

	2a (Co-1C)	2b (Ni-1C)		2b•HCl (Ni-1C-HCl)	3a (Co-2C)	3b (Ni-2C)
Bond Lengths (Å)						
P--N(2)	1.6711(19)	1.6669(17)	1.6835(17)	1.632(2)	1.6722(10)	1.6690(11)
M--P	2.4020(5)	2.3111(6)	2.3305(6)	-	2.4035(3)	2.3440(3)
M--N(1)	2.0572(16)	2.0039(17)	2.0107(16)	2.0294(19)	2.0469(10)	2.0124(10)
M--Cl(1)	2.2205(5)	2.2285(7)	2.2306(7)	2.2366(7)	2.2463(3)	2.2380(4)
M--Cl(2)	2.2558(6)	2.2312(6)	2.2350(7)	2.2264(8)	2.2460(4)	2.2424(4)
M--Cl(3)	-	-	-	2.2573(8)	-	-
N(1)--C(1)	1.346(3)	1.337(3)	1.337(3)	1.347(3)	1.3482(16)	1.3468(18)
N(1)--C(5)	1.345(3)	1.355(2)	1.352(2)	1.350(3)	1.3419(15)	1.3428(16)
C(1)--C(2)	1.384(4)	1.386(4)	1.374(3)	1.372(4)	1.375(2)	1.376(2)
C(2)--C(3)	1.348(5)	1.370(4)	1.378(3)	1.360(4)	1.370(3)	1.368(3)
C(3)--C(4)	1.380(5)	1.369(4)	1.368(3)	1.376(4)	1.373(2)	1.368(3)
C(4)--C(5)	1.392(4)	1.378(3)	1.389(3)	1.385(3)	1.3881(17)	1.3888(19)
Avg Pyridine	1.366	1.366	1.366	1.365	1.366	1.365
Bond Angles (°)						
P-M-N(1)	94.06(5)	93.59(5)	93.58(5)	-	98.07(3)	96.22(3)
M-P-N(2)	101.74(7)	103.28(7)	104.30(6)	-	112.19(4)	112.74(4)
C(7/8)-P-C(11/12)	112.18(11)	112.93(10)	112.86(11)	117.39(12)	112.19(6)	111.89(6)
Cl(1)-M-Cl(2)	110.60(2)	121.36(2)	122.64(3)	122.02(3)	109.575(15)	115.045(16)
Cl(1)-M-Cl(3)	-	-	-	108.77(3)	-	-
Cl(2)-M-Cl(3)	-	-	-	105.69(3)	-	-

Table S2: Bond lengths (Å) and angles (°) for complexes **5, 6, 7, 8,** and ligand **2=O.**

	5 (Cu-2C-Dimer)	6 (Cu-2C-CP)	7 (Cu-2C-OMe)	8 (Cu-1C-O)	2=O (1C-O)	
Bond Lengths (Å)						
P--N(2)	1.6597(9)	1.640(2)	1.621(3)	1.641(2)	1.6499(16)	1.6500(19)
P--O	1.5050(7)	1.500(2)	1.593(2)	1.4983(18)	1.4824(14)	1.4831(15)
M--P	-	-	-	-	-	-
M--N(1)	1.9876(8)	2.023(3)	2.026(3)	-	-	-
M--O	1.9364(7)	1.941(2)	-	1.9962(17)	-	-
M--Cl(1)	2.2465(3)	2.2117(12)	2.2342(10)	2.233(3)	-	-
M--Cl(2)	2.2361(3)	2.1965(10)	2.2360(10)	2.279(3)	-	-
M--Cl(3)	-	-	2.2412(9)	2.207(2)	-	-
N(1)--C(1)	1.3475(13)	1.341(4)	1.343(4)	1.344(4)	1.346(4)	1.284(16)
N(1)--C(5)	1.3524(12)	1.346(4)	1.347(4)	1.335(3)	1.341(2)	1.331(3)
C(1)--C(2)	1.3852(15)	1.378(6)	1.374(5)	1.360(5)	1.356(5)	1.43(2)
C(2)--C(3)	1.3880(17)	1.365(7)	1.374(5)	1.374(5)	1.360(5)	1.355(5)
C(3)--C(4)	1.3878(17)	1.369(5)	1.376(5)	1.379(4)	1.385(3)	1.387(4)
C(4)--C(5)	1.3922(14)	1.389(4)	1.388(4)	1.369(3)	1.369(3)	1.372(3)
Avg Pyridine	1.376	1.365	1.367	1.360	1.360	1.360
Bond Angles (°)						
O-P-N(2)	111.61(4)	108.47(12)	108.40(12)	108.15(12)	110.56(9)	110.84(8)
O-M-N(1)	143.43(3)	87.79(9)	-	-	-	-
C(7/8)-P-C(11/12)	114.43(5)	115.34(16)	115.75(15)	116.25(14)	114.17(10)	114.00(10)
Cl(1)-M-Cl(2)	142.477(11)	99.14(5)	99.50(4)	104.33(18)	-	-
Cl(1)-M-Cl(3)	-	-	134.49(5)	103.41(11)	-	-
Cl(2)-M-Cl(3)	-	-	98.94(4)	114.4(2)	-	-

Table S3: Crystallographic data and refinement parameters for complexes **2a, 2b, 3a,** and **3b.**

Description	**2a (Co-1C)**	**2b (Ni-1C)**	**3a (Co-2C)**	**3b (Ni-2C)**
Empirical Formula	C_{14} H_{25} Cl_2 N_2 Co P	C_{14} H_{25} Cl_2 N_2 Ni P	C_{15} H_{27} Cl_2 N_2 Co P	C_{15} H_{27} Cl_2 N_2 Ni P
Formula Weight	382.16	381.94	396.18	395.96
Wavelength (Å)	0.71073	0.71073	0.71073	0.71073
Temperature (K)	293(2)	293(2)	293(2)	293(2)
Crystal system	Orthorhombic	Monoclinic	Monoclinic	Monoclinic
Space Group	$P2_12_12_1$	$P2_1/n$	$P2_1/n$	$P2_1/n$
a (Å)	10.5503(2)	13.3712(10)	8.8055(2)	8.8054(3)
b (Å)	11.6343(2)	12.0474(9)	15.0416(3)	15.0567(6)
c (Å)	14.8131(3)	23.5918(18)	14.6897(3)	14.6029(5)
α (°)	90	90	90	90
β (°)	90	104.837(4)	98.7060(10)	99.846(2)
γ (°)	90	90	90	90
V (Å^3)	1818.24(6)	3673.6(5)	1923.22(7)	1907.54(12)
Z	4	8	4	4
Density (g/cm^3)	1.396	1.381	1.368	1.379
μ (mm^{-1})	1.318	1.427	1.249	1.377
F (000)	796	1600	828	832
Θ min., max. (°)	2.226, 32.806	1.600, 27.528	1.949, 32.814	1.958, 31.732
Crystal size (mm)	0.10 x 0.12 x 0.93	0.08 x 0.19 x 0.24	0.25 x 0.31 x 0.54	0.16 x 0.52 x 0.56
Index ranges	-15 < h < 15; -17 < k < 17; -22 < l < 22	-17 < h < 17; -15 < k < 15; -30 < l < 30	-13 < h < 13; -22 < k < 22; -22 < l < 21	-12 < h < 13; -22 < k < 22; -21 < l < 21
Reflections collected	32966	49071	34792	34307
R_{int} (%)	0.0179	0.0300	0.0161	0.0199
Data/restraints/parameters	6389/3/190	8444/6/379	6773/3/199	6451/3/199
Goodness-of-fit on F^2	1.051	1.014	1.037	1.027
R_1 [I > 2σ(I)]	0.0257	0.0316	0.0270	0.0280
wR_2 [I > 2σ(I)]	0.0707	0.0869	0.0790	0.0778
Largest diff. peak/hole (e Å^{-3})	0.734 and -0.236	0.647 and -0.312	0.558 and -0.445	0.622 and -0.373
Observed data [I > 2.0σ(I)]	5802	6409	5815	5423

Table S4: Crystallographic data and refinement parameters for complexes **5, 6, 7,** and **8.**

Description	**5 (Cu-2C-O-Dimer)**	**6 (Cu-2C-O-Polymer)**	**7 (Cu-2C-OMe)**	**8 (Cu-1C-O)**
Empirical Formula	C_{30} H_{54} Cl_4 N_4 Cu_2 O_2 P_2	C_{15} H_{27} Cl_2 N_2 Cu O P	C_{16} H_{30} Cl_3 N_2 Cu O P	C_{14} H_{26} Cl_3 N_2 Cu O P [+ 2 (H_2 O)]
Formula Weight	833.59	416.79	467.28	439.23
Wavelength (Å)	0.71073	0.71073	0.71073	0.71073
Temperature (K)	293(2)	293(2)	293(2)	293(2)
Crystal system	Triclinic	Monoclinic	Monoclinic	Monoclinic
Space Group	*P*-1	*C*c	$P2_1$/n	$P2_1$/c
a (Å)	8.3490(4)	9.670(4)	8.4135(2)	14.14310(10)
b (Å)	11.6402(6)	24.423(9)	13.9973(3)	8.98120(10)
c (Å)	11.6734(6)	8.680(3)	17.9874(3)	17.4366(2)
α (°)	110.5230(10)	90	90	90
β (°)	101.0310(10)	102.684(9)	92.0770(10)	101.1680(10)
γ (°)	109.1720(10)	90	90	90
V (Å^3)	941.38(8)	2000.0(14)	2116.92(8)	2172.89(4)
Z	1	4	4	4
Density (g/cm^3)	1.470	1.384	1.466	1.343
μ (mm^{-1})	1.531	1.441	1.492	1.449
F (000)	434	868	972	908
Θ min., max. (°)	2.069, 32.789	1.668, 35.563	1.844, 27.504	1.468, 32.871
Crystal size (mm)	0.18 x 0.43 x 0.62	0.09 x 0.27 x 0.62	0.08 x 0.15 x 0.22	0.26 x 0.36 x 0.50
Index ranges	-12 < h < 12; -17 < k < 17; -17 < l < 17	-15 < h < 15; -39 < k < 39; -14 < l < 14	-10 < h < 10; -18 < k < 18; -23 < l < 23	-20 < h < 20; -13 < k < 13; -26 < l < 26
Reflections collected	12243	42015	26748	37317
R_{int} (%)	0.0155	0.0357	0.0680	0.0189
Data/restraints/parameters	6271/3/208	8823/5/209	4858/3/227	7671/15/241
Goodness-of-fit on F^2	1.032	1.022	1.016	1.046
R_1 [I > 2σ(I)]	0.0203	0.0398	0.0412	0.0485
wR_2 [I > 2σ(I)]	0.0567	0.0949	0.0984	0.1462
Largest diff. peak/hole (e Å^{-3})	0.513 and -0.443	0.577 and -0.277	0.428 and -0.458	0.586 and -0.626
Observed data [I > 2.0σ(I)]	5880	6473	3137	5818

Table S5: Crystallographic data and refinement parameters for ligand **2=O**, compound **4**, complexes **2b•HCl** and **9.**

Description	**2=O**	**2b•HCl (Ni-1C-HCl)**	**4 (BHT-1C)**	**9 (Ag-2C)**
Empirical Formula	C_{14} H_{25} N_2 O P	C_{14} H_{26} Cl_3 N_2 Ni P	C_{23} H_{41} N O P, Cl	C_{60} H_{108} Cl_2 N_8 Ag_4 P_4, 2(B F_4)
Formula Weight	268.33	418.40	413.99	1741.42
Wavelength (Å)	0.71073	0.71073	0.71073	0.71073
Temperature (K)	293(2)	293(2)	150(2)	293(2)
Crystal system	Monoclinic	Orthorhombic	Monoclinic	Triclinic
Space Group	$P2_1/n$	$Pbca$	$P2_1/c$	P-1
a (Å)	11.509(8)	15.5512(8)	11.8979(4)	12.3096(2)
b (Å)	22.039(16)	14.6926(7)	16.6511(5)	12.3824(2)
c (Å)	13.238(10)	16.9036(9)	12.3939(4)	13.0675(2)
α (°)	90	90	90	77.1240(10)
β (°)	106.946(19)	90	94.159(2)	84.4990(10)
γ (°)	90	90	90	88.5690(10)
V (Å^3)	3212(4)	3862.3(3)	2448.93(14)	1932.74(5)
Z	8	8	4	1
Density (g/cm^3)	1.110	1.439	1.123	1.496
μ (mm^{-1})	0.164	1.498	0.234	1.209
F (000)	1168	1744	904	888
ϴ min., max. (°)	1.853, 29.391	2.256, 27.707	2.052, 33.115	1.662, 32.937
Crystal size (mm)	0.10 x 0.20 x 1.80	0.19 x 0.27 x 0.32	0.43 x 0.43 x 0.44	0.07 x 0.19 x 0.35
Index ranges	-15 < h < 15; -29 < k < 29; -17 < l < 17	-20 < h < 20; -19 < k < 19; -22 < l < 21	-18 < h < 18; -25 < k < 25; -18 < l < 18	-18 < h < 18; -18 < k < 18; -19 < l < 19
Reflections collected	48890	47142	42990	34628
R_{int} (%)	0.0321	0.0556	0.0268	0.0207
Data/restraints/parameters	8391/0/359	4434/4/203	8770/4/303	13342/76/461
Goodness-of-fit on F^2	1.035	1.066	1.042	1.046
R_1 [I > 2σ(I)]	0.0481	0.0354	0.0372	0.0302
wR_2 [I > 2σ(I)]	0.1494	0.0998	0.1066	0.0765
Largest diff. peak/hole (e Å^{-3})	0.349 and -0.198	0.497 and -0.520	0.721 and -0.318	0.481 and -0.467
Observed data [I > 2.0σ(I)]	5581	3580	7515	9625

UV-Vis Spectra

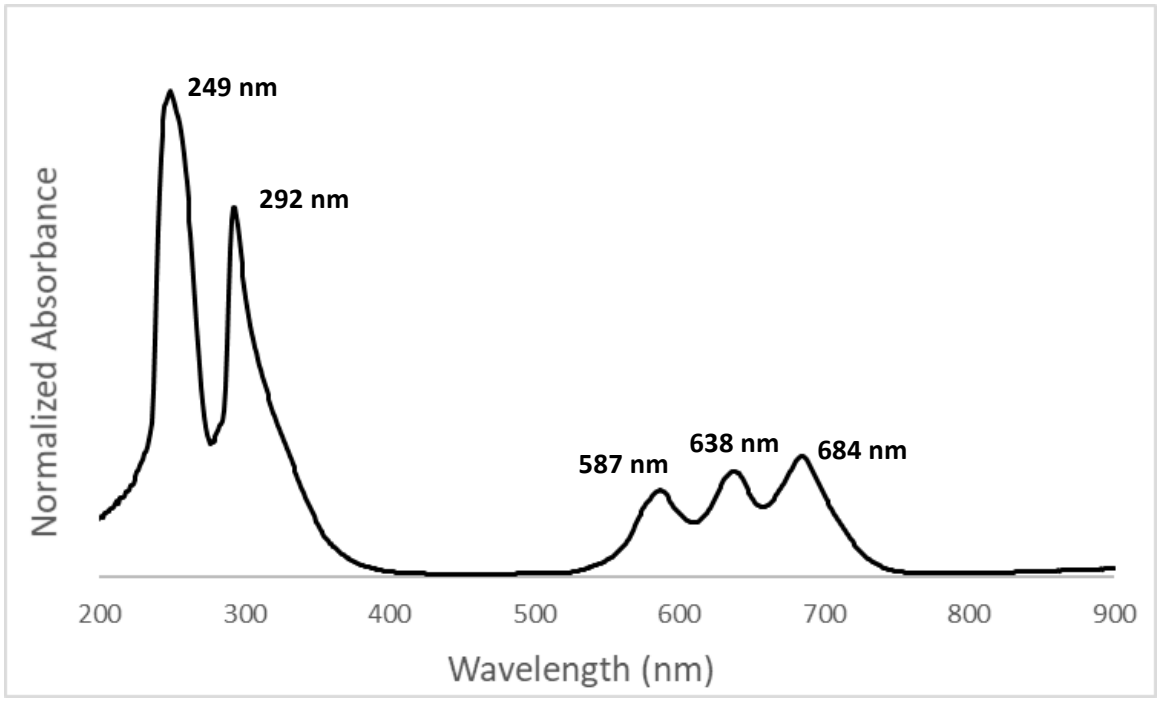

Figure S27: UV-Vis spectrum of Co(II) complex **2a** in tetrahydrofuran.

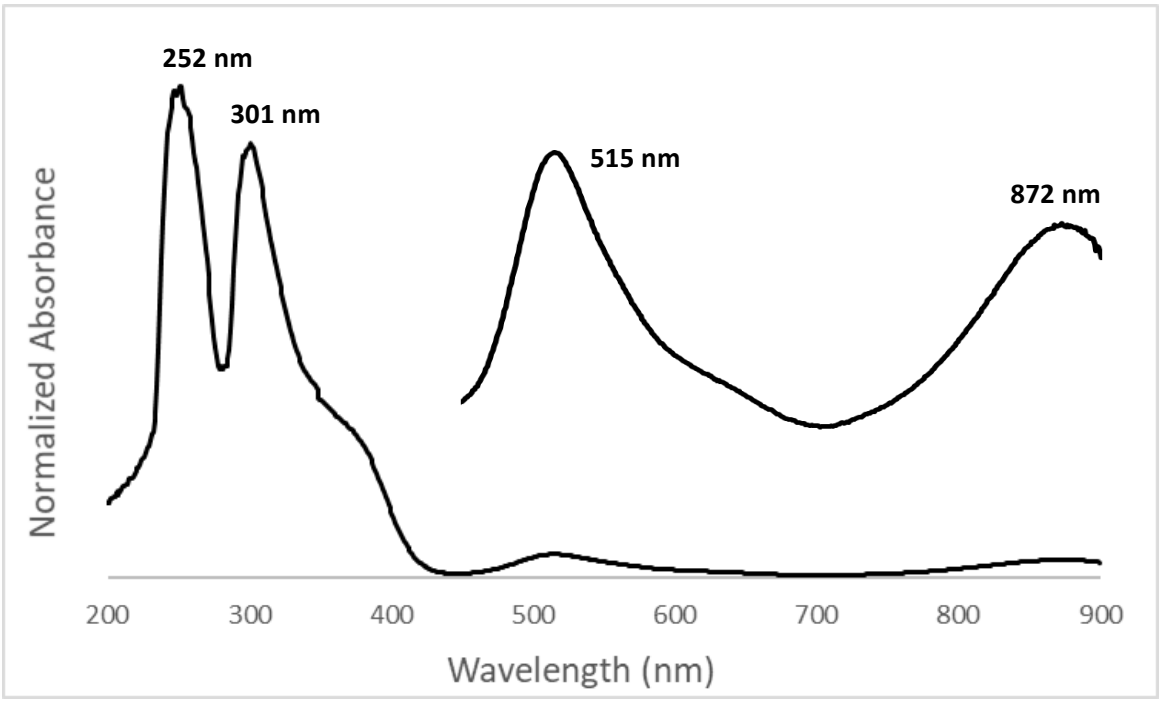

Figure S28: UV-Vis spectrum of Ni(II) complex **2b** in tetrahydrofuran.

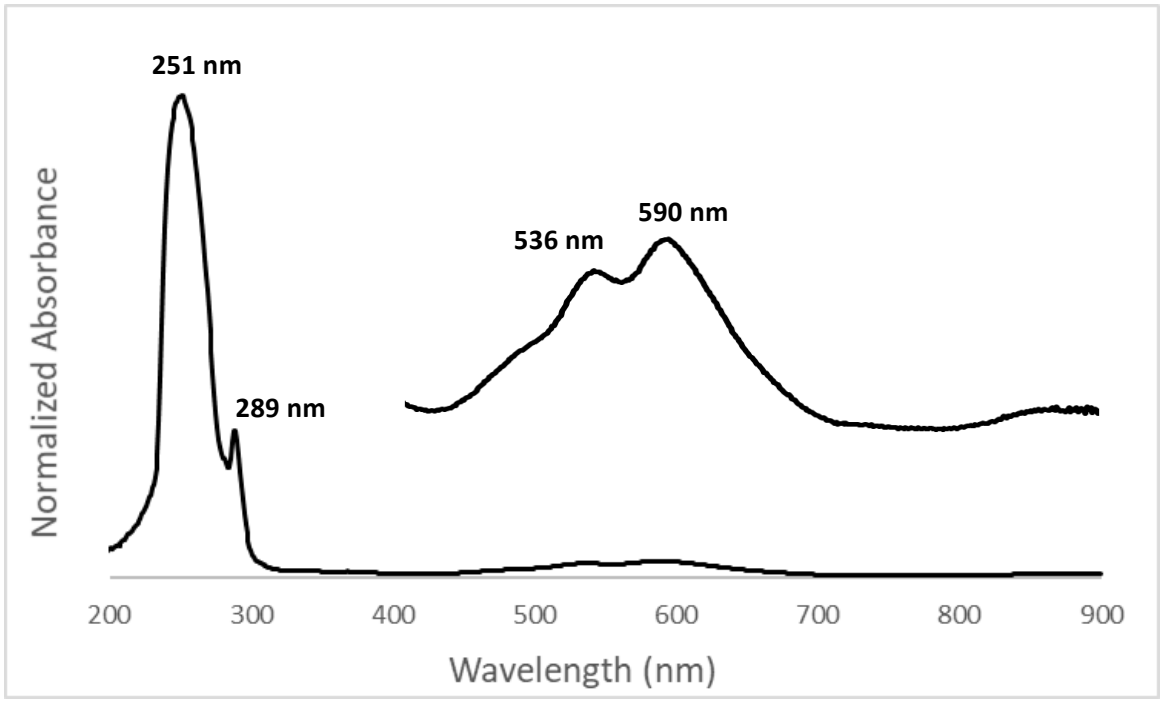

Figure S29: UV-Vis spectrum of HCl activated Ni(II) complex **2b•HCl** in tetrahydrofuran.

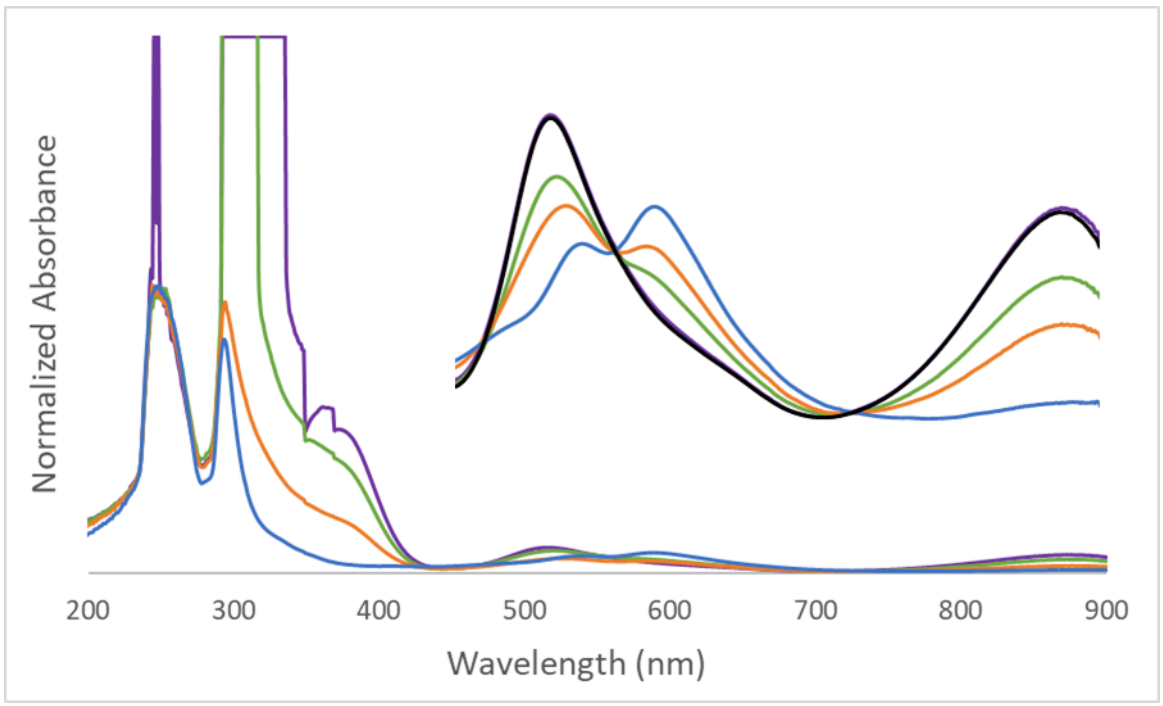

Figure S30: UV-Vis spectra of unanticipated "HCl" addition into **2b** on Day 1 (purple), Day 2 (green), Day 3 (orange), Day 4 - **2b•HCl** (blue). Inset shows zoomed-in spectra from 450-900 nm; Day 21 after additional synthesis purification (black).

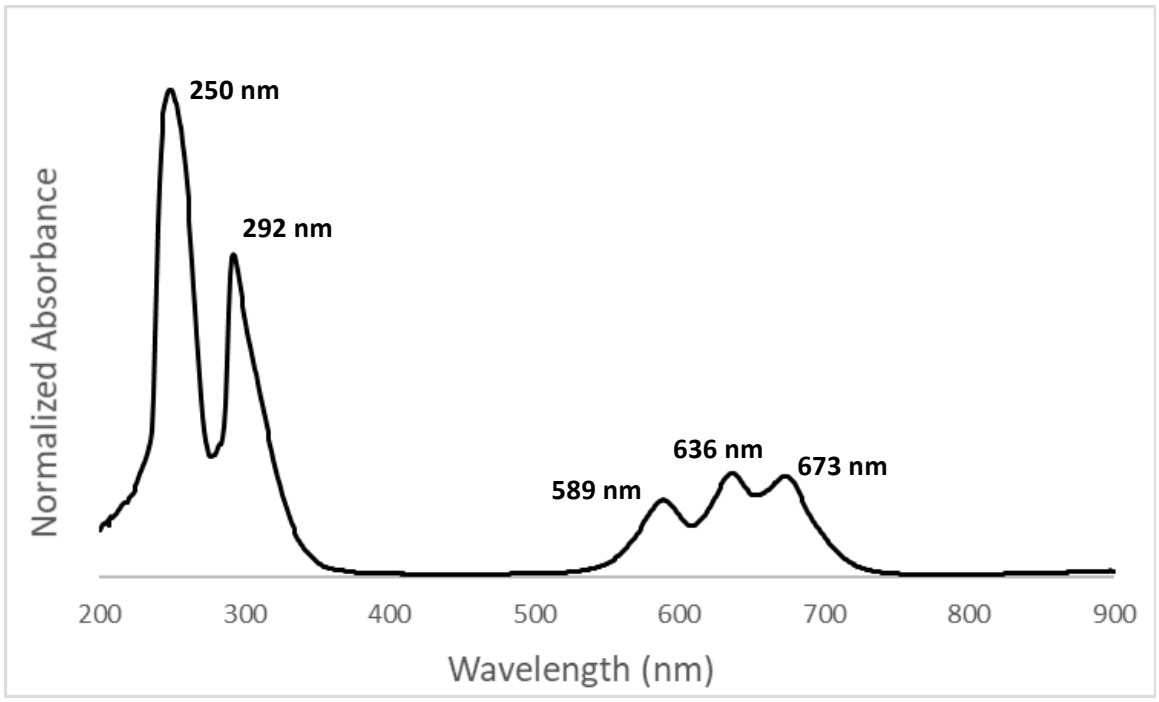

Figure S31: UV-Vis spectrum of Co(II) complex **3a** in tetrahydrofuran.

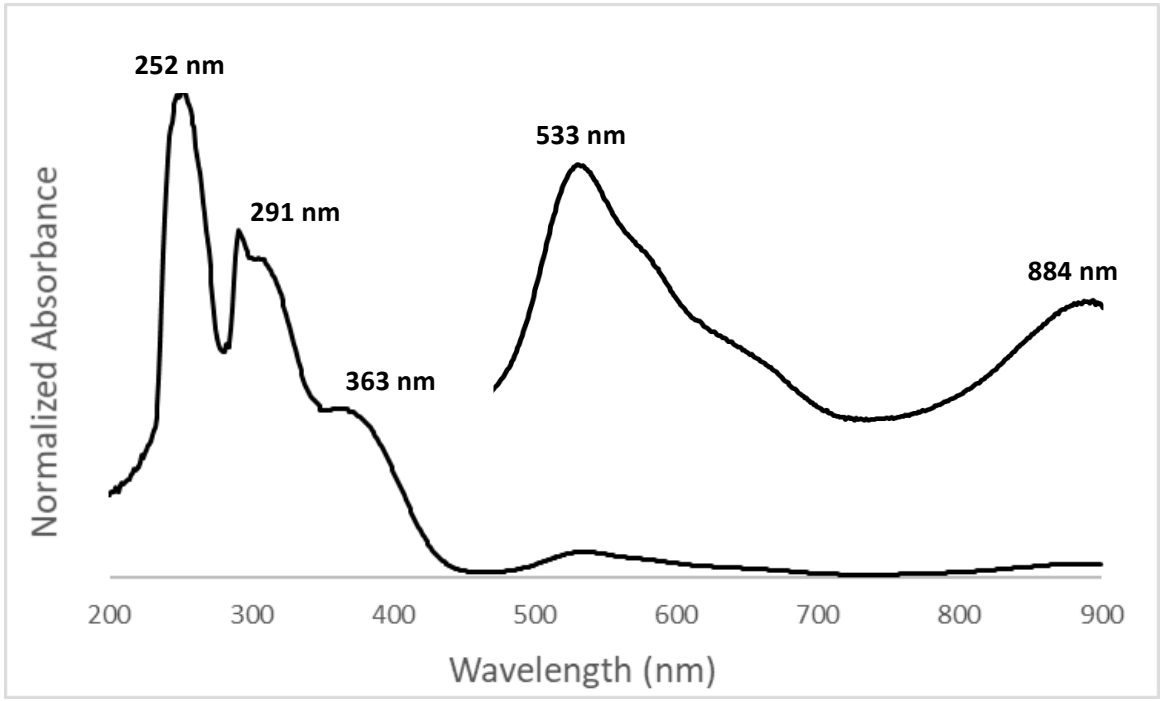

Figure S32: UV-Vis spectrum of Ni(II) complex **3b** in tetrahydrofuran.

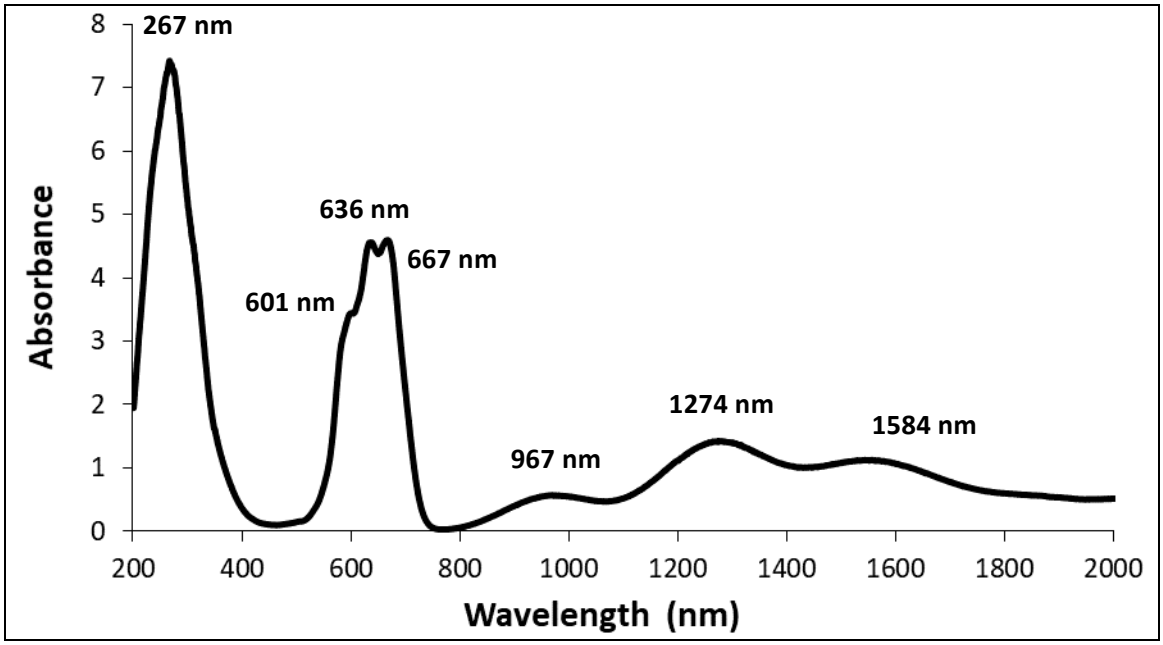

Figure S33: Solid-state UV-Vis spectrum of Co(II) complex **2a**.

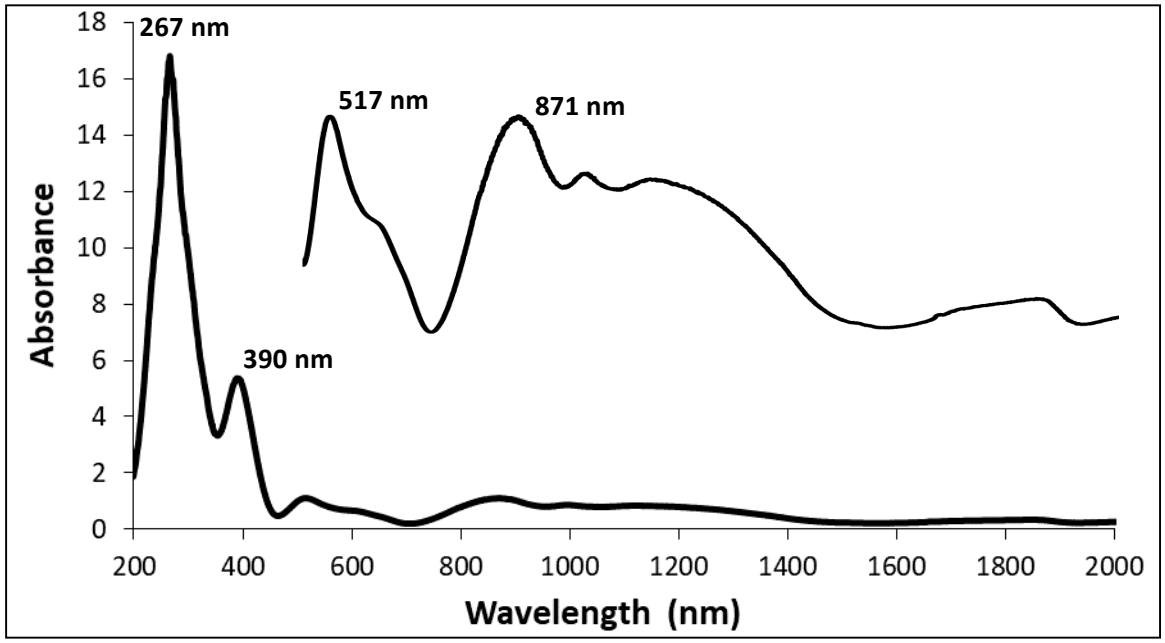

Figure S34: Solid-state UV-Vis spectrum of Ni(II) complex **2b**.

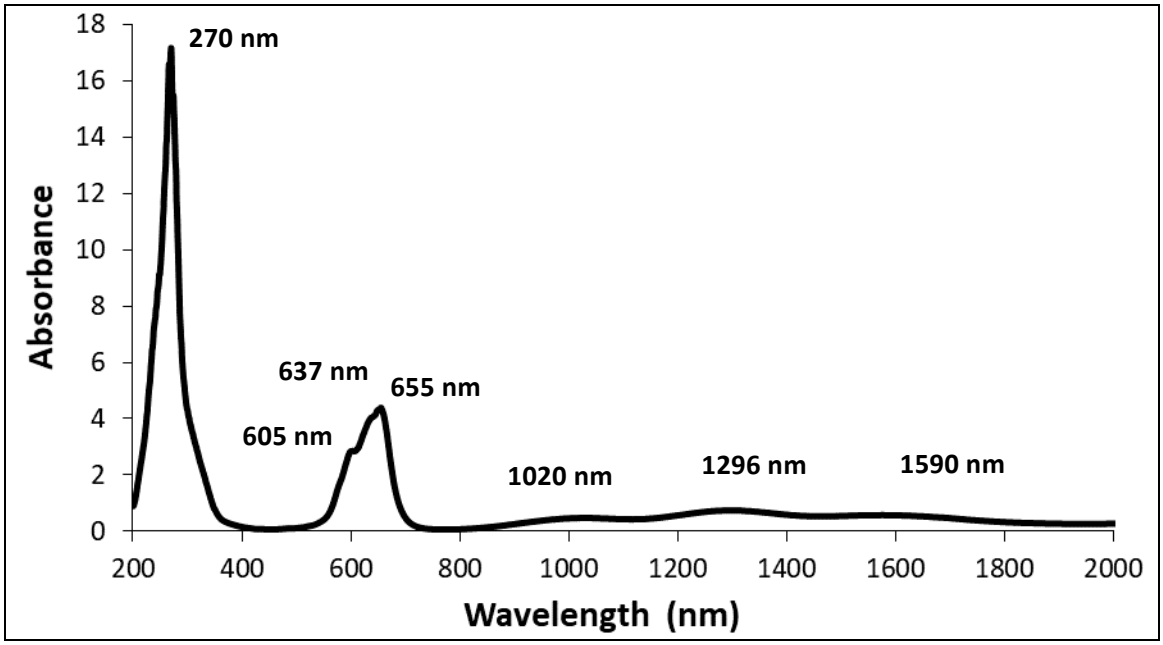

Figure S35: Solid-state UV-Vis spectrum of Co(II) complex **3a**.

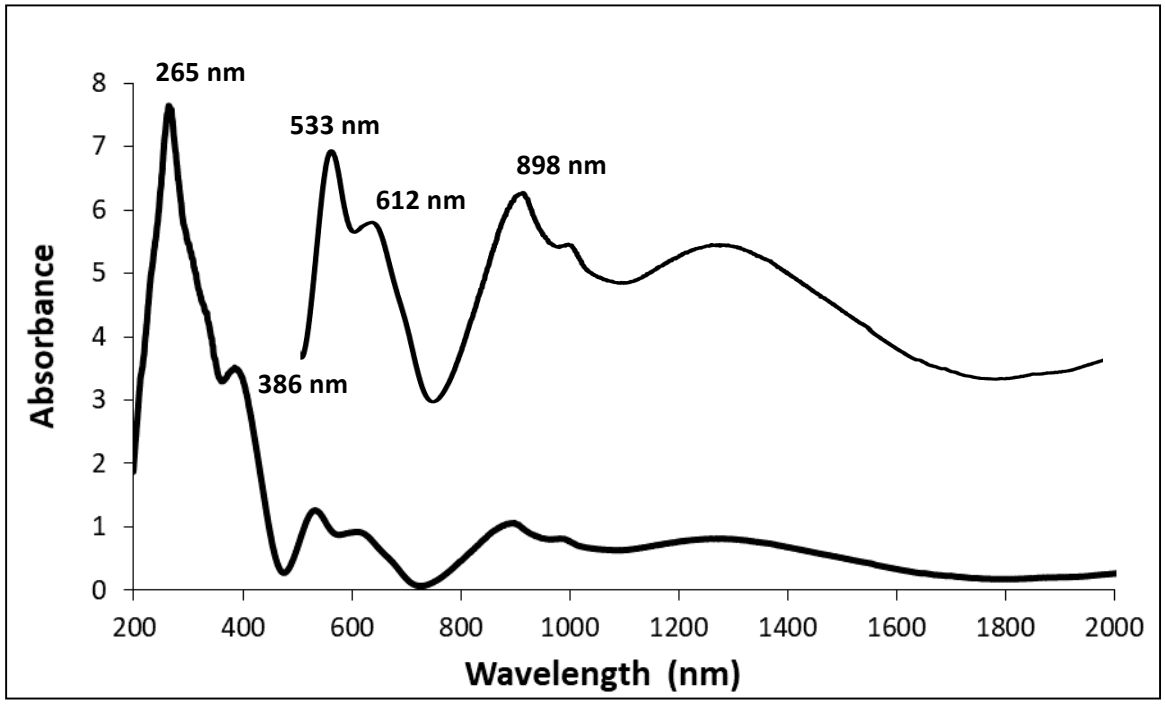

Figure S36: Solid-state UV-Vis spectrum of Ni(II) complex **3b**.